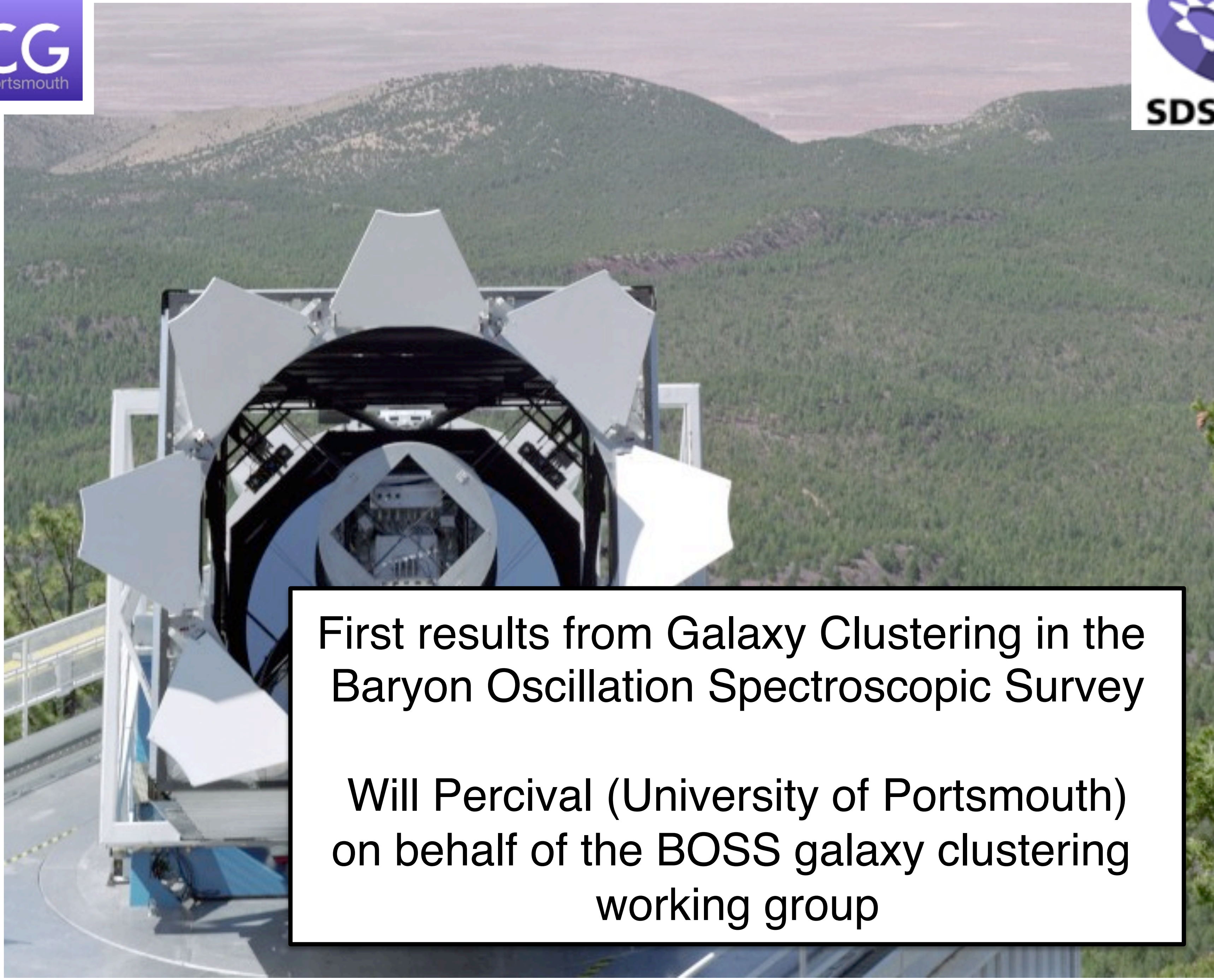

First results from Galaxy Clustering in the Baryon Oscillation Spectroscopic Survey

Will Percival (University of Portsmouth)
on behalf of the BOSS galaxy clustering working group

Cosmology from Spectroscopic Galaxy Surveys

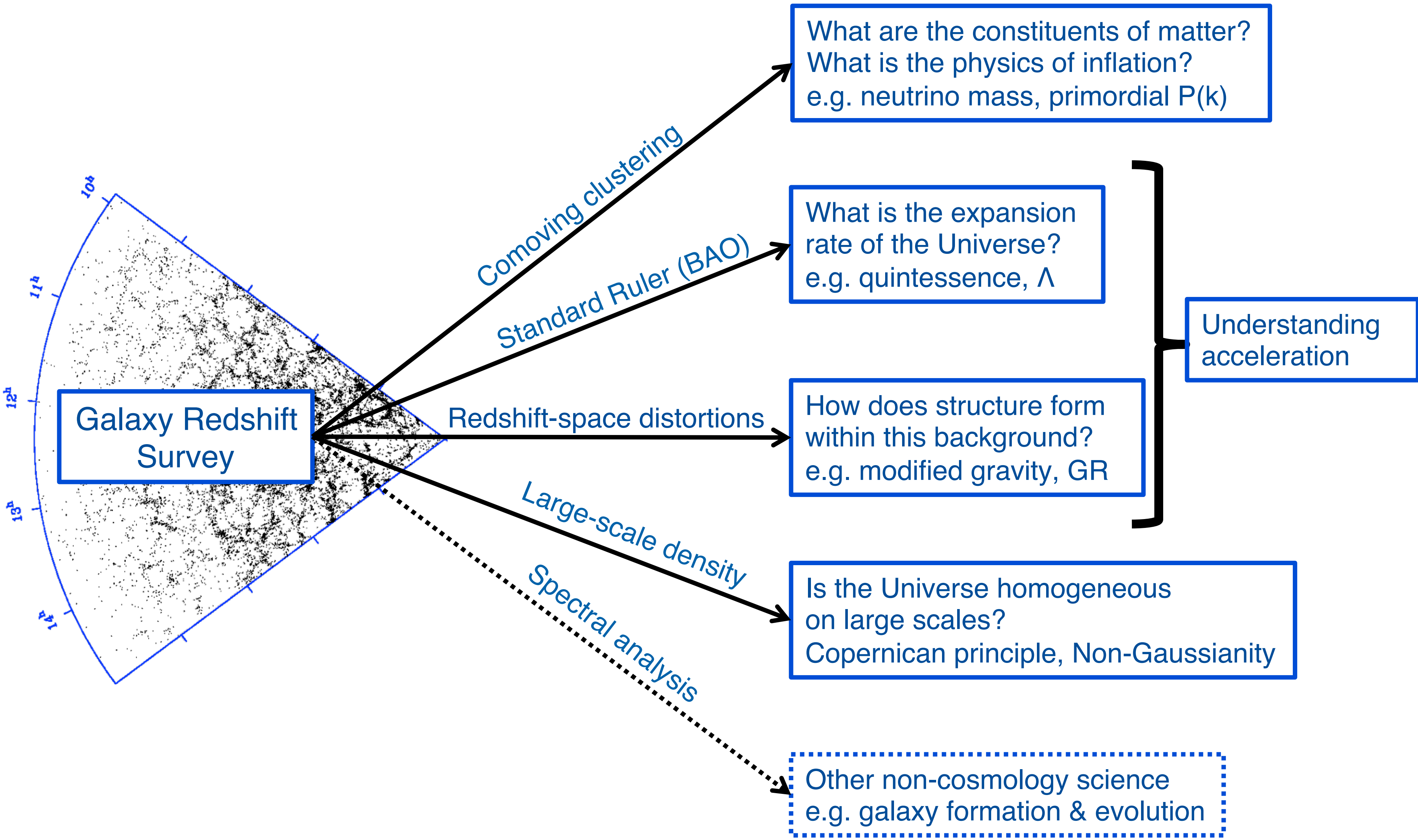

What does “galaxy clustering” mean?

Clustering strength = number of galaxy pairs beyond random

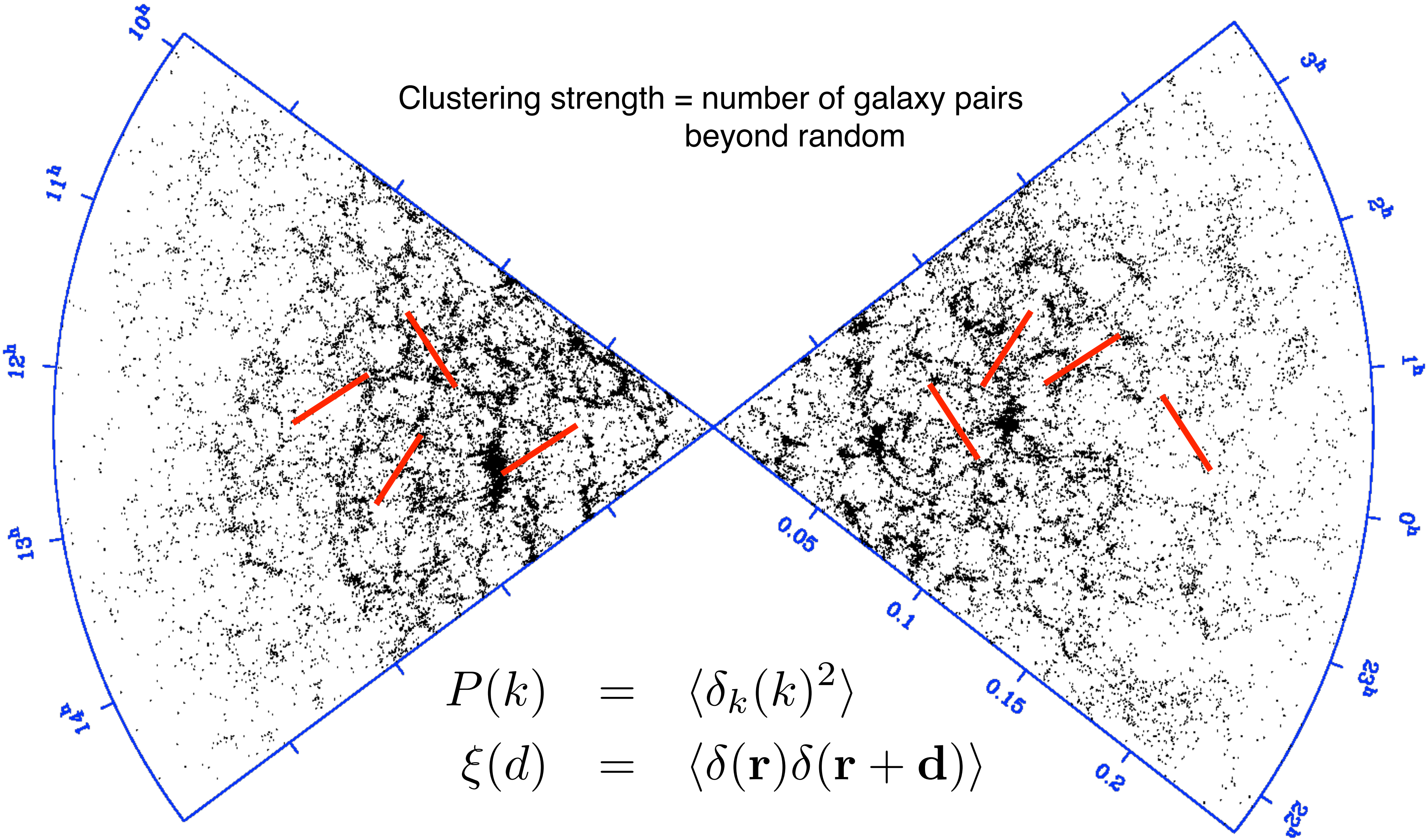

$$P(k) = \langle \delta_k(k)^2 \rangle$$

$$\xi(d) = \langle \delta(\mathbf{r})\delta(\mathbf{r}+\mathbf{d}) \rangle$$

2dFGRS

Correlation function (preview)

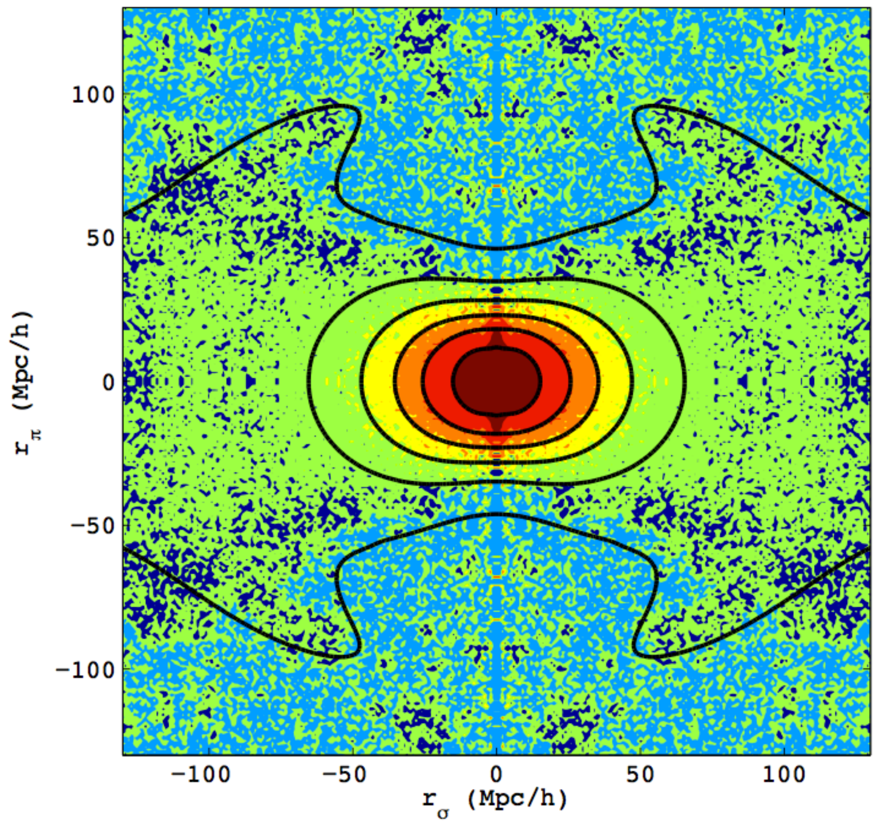

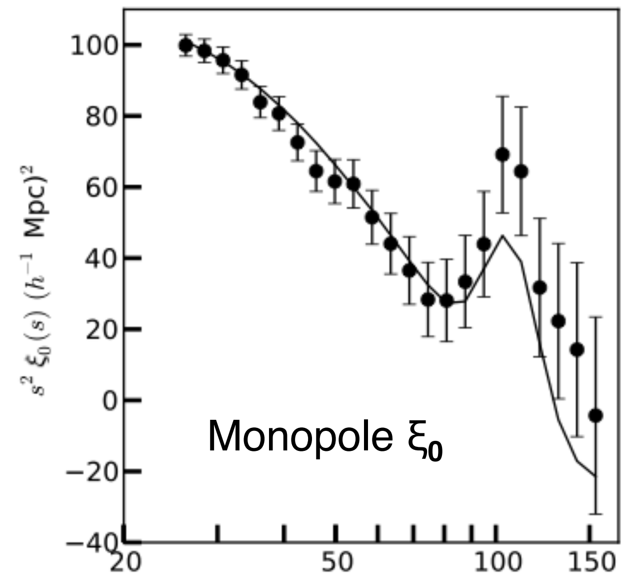

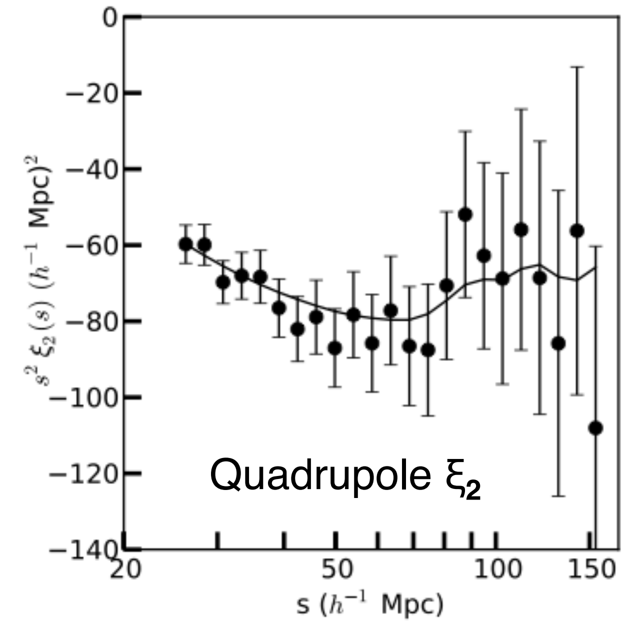

$$\xi_0(s) = \int_0^1 d\mu\,\xi(s,\mu)$$

$$\xi_2(s) = 5\int_0^1 d\mu\,\xi(s,\mu)L_2(\mu)$$

Power spectrum (preview)

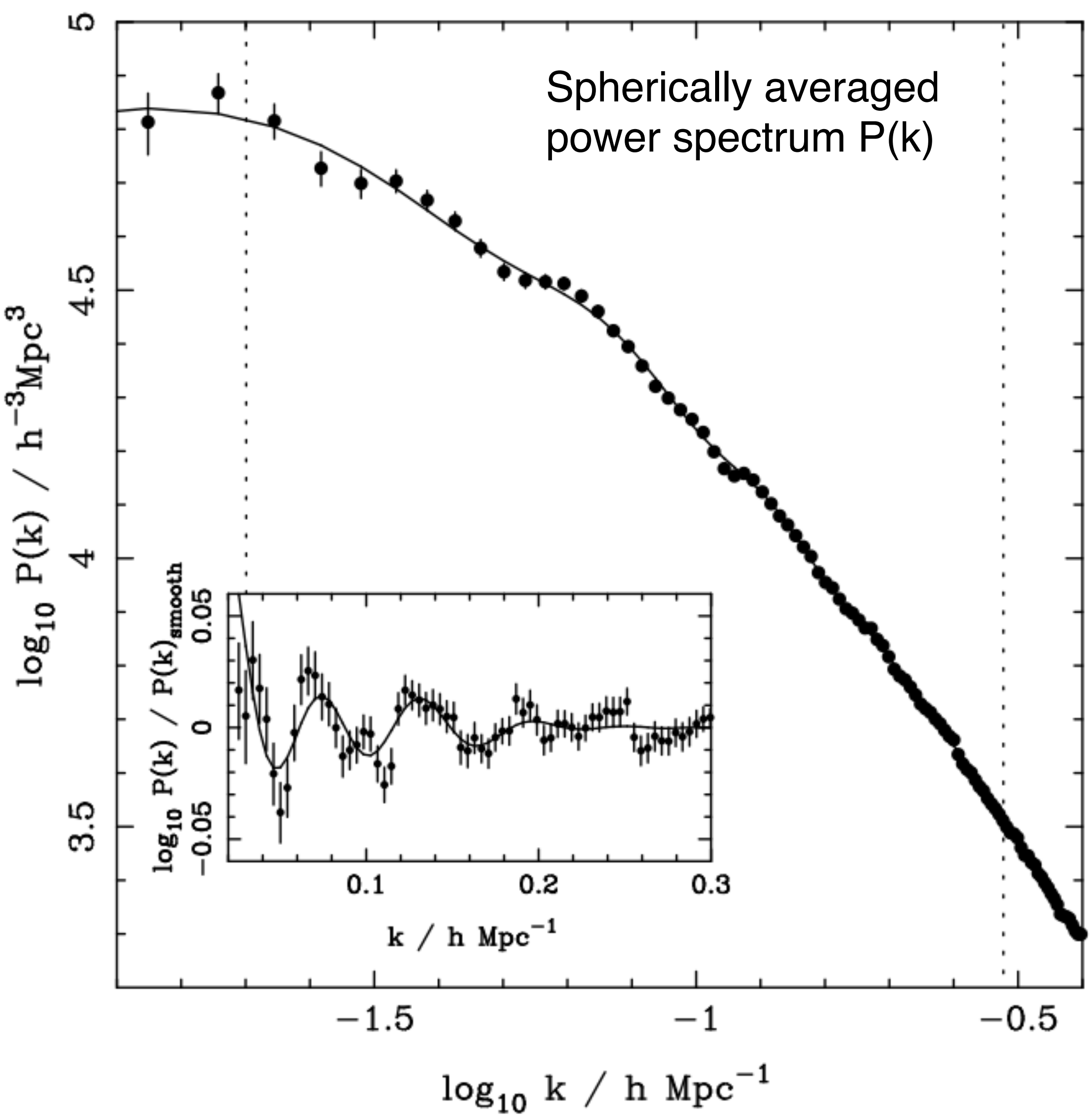

The BOSS survey

BOSS summary

- Duration: Fall 2009 - Summer 2014, dark time
- Telescope: 2.5m Sloan
- Upgrade to SDSS-II spectrograph
  - 1000 smaller fibers
  - higher throughput
- Spectra:
  - 3600 Å < λ < 10,000 Å New spectrograph
  - $R = \lambda/\Delta\lambda = 1300 - 3000$
  - (S/N) at mag. limit
    - 22 per pix. (averaged over 7000-8500Å)
    - 10 per pix. (averaged over 4000-5500Å)
- Area: 10,000 deg2
- Targets:
  - 1.5×10^6 massive galaxies, $z < 0.7$, $i < 19.9$
  - 1.5×10^5 quasars, $z>2.2$, $g<22.0$ selected from 4×10^5 candidates
  - 75,000 ancillary science targets, many categories
- Measurements from Galaxies:
  - $d_A(z)$ to 1.2% at $z = 0.35$ and 1.2% $z = 0.6$
  - $H(z)$ to 2.2% at $z = 0.35$ and 2.0% at $z = 0.6$
- Measurements from Lyα Forest:
  - $d_A(z)$ to 4.5% at $z = 2.5$ $H(z)$ to 2.6% at $z = 2.5$

132 pages of science

- **Anderson et al.** (alphabetical) arXiv:1203.6565 - BAO measurement in power-spectrum and correlation function.
- **Reid et al.** arXiv:1203.6641- Anisotropic clustering, redshift-space distortion measurements.
- **Sanchez et al.** arXiv:1203.6616 - Fits to the full shape of the correlation function.
- **Ross et al.** arXiv:1203.6499 - Large-scale systematics.
- **Manera et al.** arXiv:1203.6609 - 600 PTHalo mocks.
- **Tojeiro et al.** arXiv:1203.6565 - Enhanced redshift-space distortion measurements.

- Plus more to come soon …

The cast …

Lauren Anderson[1], Eric Aubourg[2], Stephen Bailey[3], Dmitry Bizyaev[4], Michael Blanton[5], Adam S. Bolton[6], J. Brinkmann[4], Joel R. Brownstein[6], Angela Burden[7], Antonio J. Cuesta[8], Luiz N. A. da Costa[9,10], Kyle S. Dawson[6], Roland de Putter[11,12], Daniel J. Eisenstein[13], James E. Gunn[14], Hong Guo[15], Jean-Christophe Hamilton[2], Paul Harding[15], Shirley Ho[3,14], Klaus Honscheid[16], Eyal Kazin[17], D. Kirkby[18], Jean-Paul Kneib[19], Antione Labatie[20], Craig Loomis[21], Robert H. Lupton[14], Elena Malanushenko[4], Viktor Malanushenko[4], Rachel Mandelbaum[14,21], Marc Manera[7], Claudia Maraston[7], Cameron K. McBride[13], Kushal T. Mehta[22], Olga Mena[11], Francesco Montesano[23], Demetri Muna[5], Robert C. Nichol[7], Sebastián E. Nuza[24], Matthew D. Olmstead[6], Daniel Oravetz[4], Nikhil Padmanabhan[8], Nathalie Palanque-Delabrouille[25], Kaike Pan[4], John Parejko[8], Isabelle Pâris[26], Will J. Percival[7], Patrick Petitjean[26], Francisco Prada[27,28,29], Beth Reid[3,30], Natalie A. Roe[3], Ashley J. Ross[7], Nicholas P. Ross[3], Lado Samushia[7,31], Ariel G. Sánchez[23], David J. Schlegel[*3], Donald P. Schneider[32,33], Claudia G. Scóccola[34,35], Hee-Jong Seo[36], Erin S. Sheldon[37], Audrey Simmons[4], Ramin A. Skibba[22], Michael A. Strauss[21], Molly E. C. Swanson[13], Daniel Thomas[7], Jeremy L. Tinker[5], Rita Tojeiro[7], Mariana Vargas Magaña[2], Licia Verde[38], Christian Wagner[12], David A. Wake[39], Benjamin A. Weaver[5], David H. Weinberg[40], Martin White[3,41,42], Xiaoying Xu[22], Christophe Yèche[25], Idit Zehavi[15], Gong-Bo Zhao[7,43]

Anderson et al.

Galaxy distribution

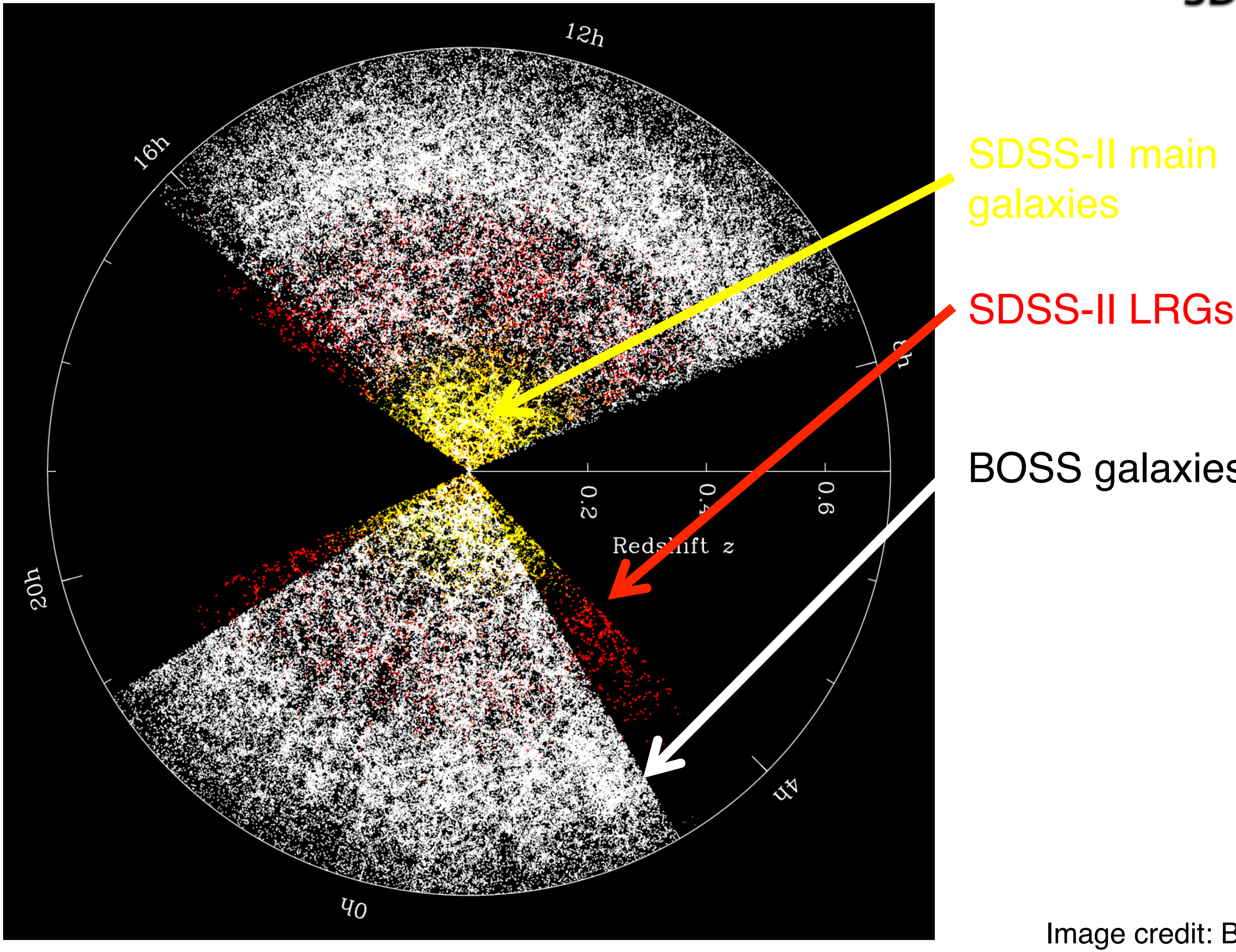

Image credit: Blanton

The CMASS galaxy sample

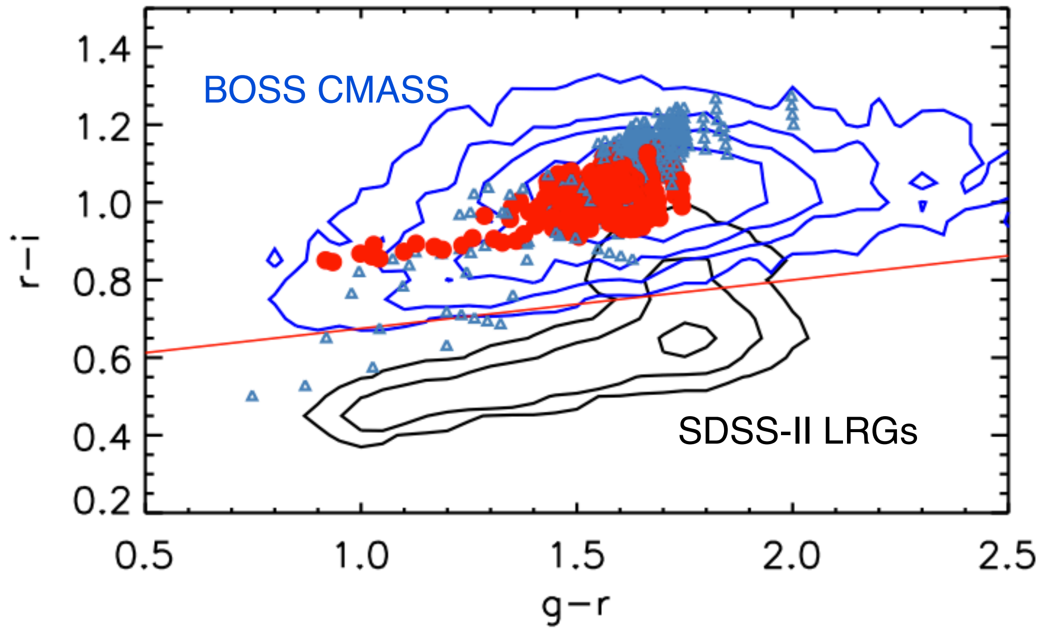

Standard colour selection criteria

$$
\begin{aligned}
17.5 < i_{\rm cmod} &< 19.9,\\
r_{\rm mod} - i_{\rm mod} &< 2.0,\\
d_{\perp} &> 0.55,\\
i_{\rm fib2} &< 21.5,\\
i_{\rm cmod} &< 19.86 + 1.6(d_{\perp} - 0.8),
\end{aligned}
$$

$$d_{\perp} = r_{\rm mod} - i_{\rm mod} - (g_{\rm mod} - r_{\rm mod})/8.0$$

Extends SDSS-II LRG cuts to cover both blue and red massive galaxies at higher redshifts

Also include star-galaxy separation criteria

$$
\begin{aligned}
i_{\rm psf} - i_{\rm mod} &> 0.2 + 0.2(20.0 - i_{\rm mod}),\\
z_{\rm psf} - z_{\rm mod} &> 9.125 - 0.46 z_{\rm mod},
\end{aligned}
$$

Galaxy distribution: DR9

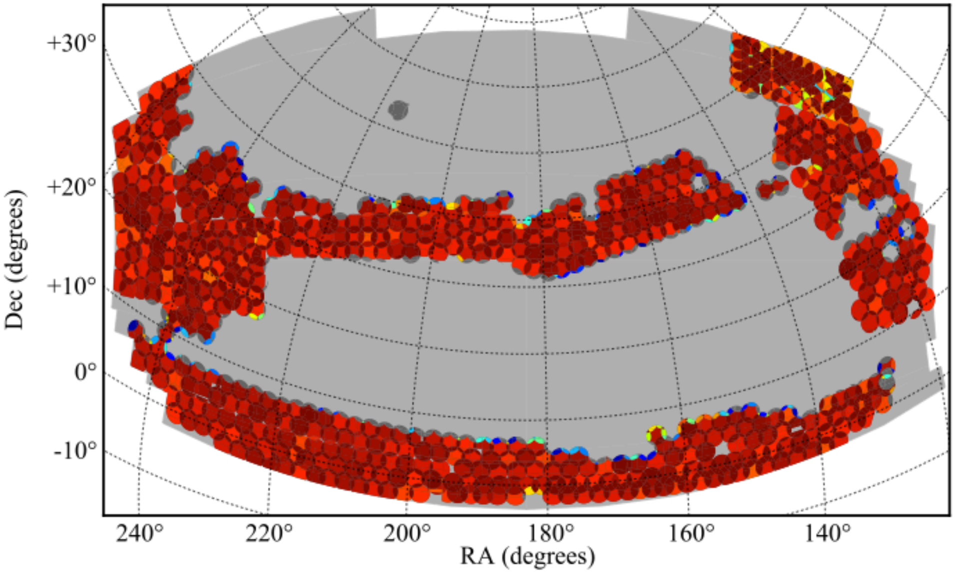

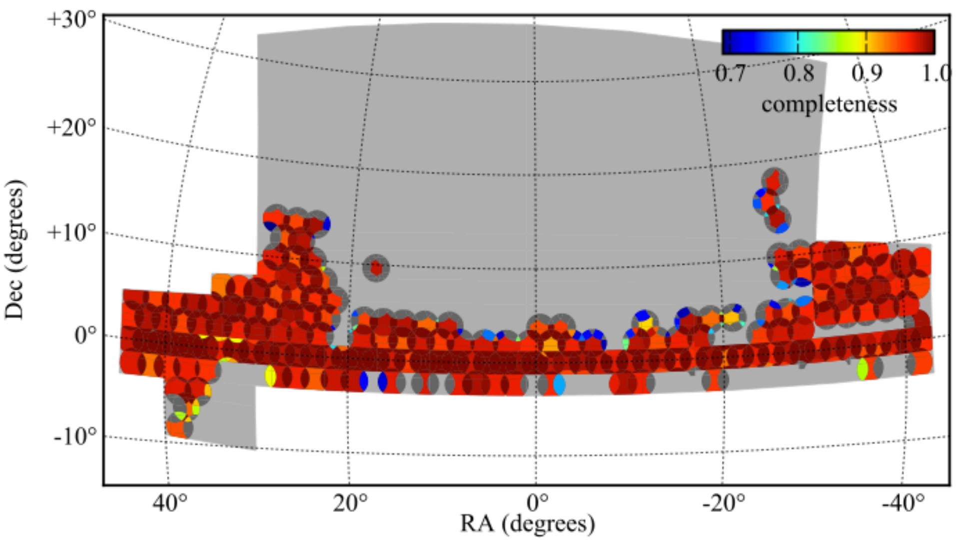

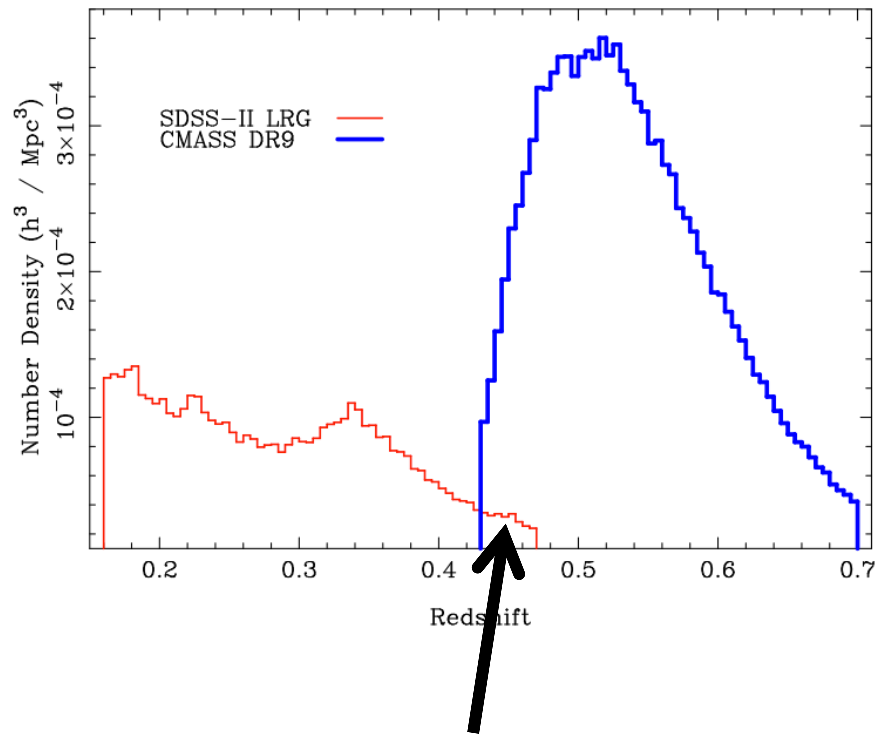

Some of the CMASS galaxies already have known redshifts

The catalogue

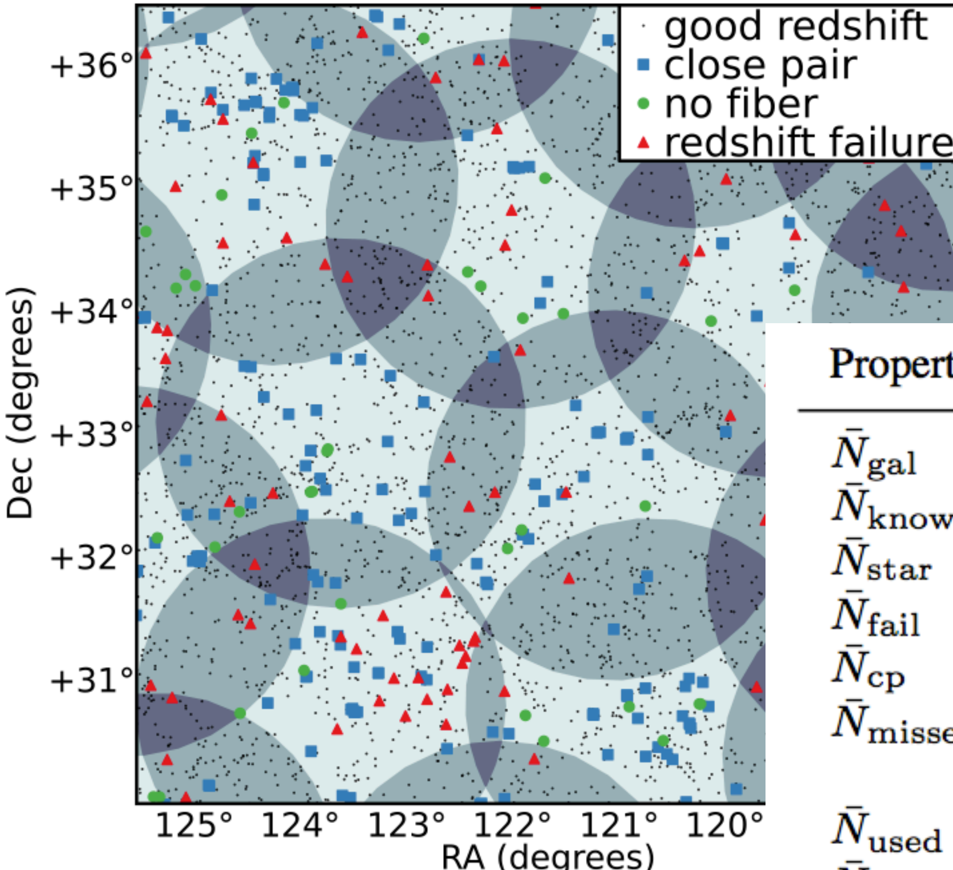

Property	NGC	SGC	total
$\bar{N}_{\rm gal}$	222 538	60 792	283 330
$\bar{N}_{\rm known}$	3766	1810	5576
$\bar{N}_{\rm star}$	7201	1771	8972
$\bar{N}_{\rm fail}$	3751	1122	4873
$\bar{N}_{\rm cp}$	14 116	3640	17 756
$\bar{N}_{\rm missed}$	4931	1911	6842
$\bar{N}_{\rm used}$	207 246	57 037	264 283
$\bar{N}_{\rm obs}$	233 490	63 685	297 175
$\bar{N}_{\rm targ}$	256 303	71 046	327 349
Total area / deg^2	2635	709	3344
Effective area / deg^2	2584	690	3275

Anderson et al.; Ross et al.

Redshift failures & close pairs

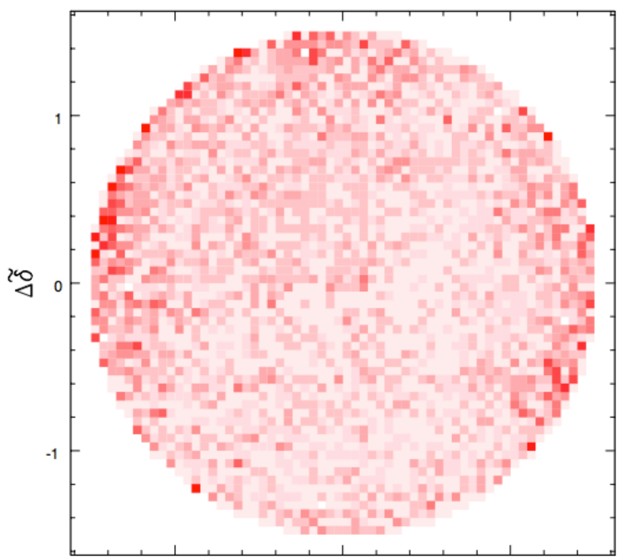

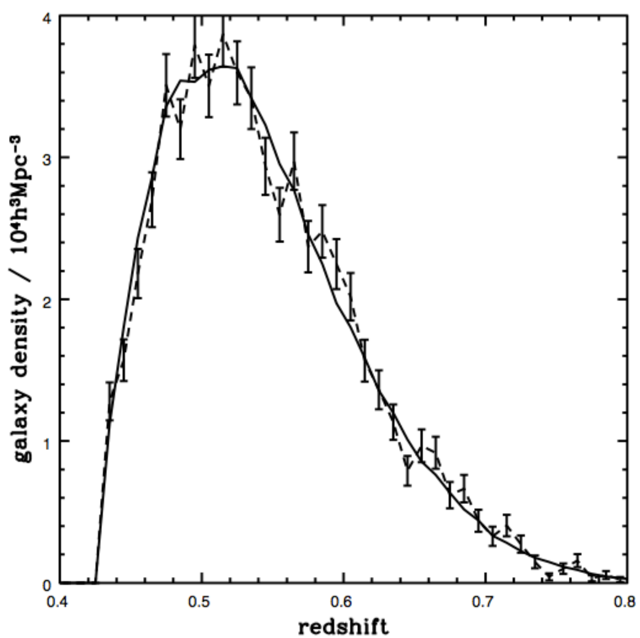

- Spectra where we failed to get an accurate redshift are spatially correlated
- Close pairs obviously correlated with density
- Correct both by upweighting the nearest target with good classification

Ross et al.

Target density fluctuations

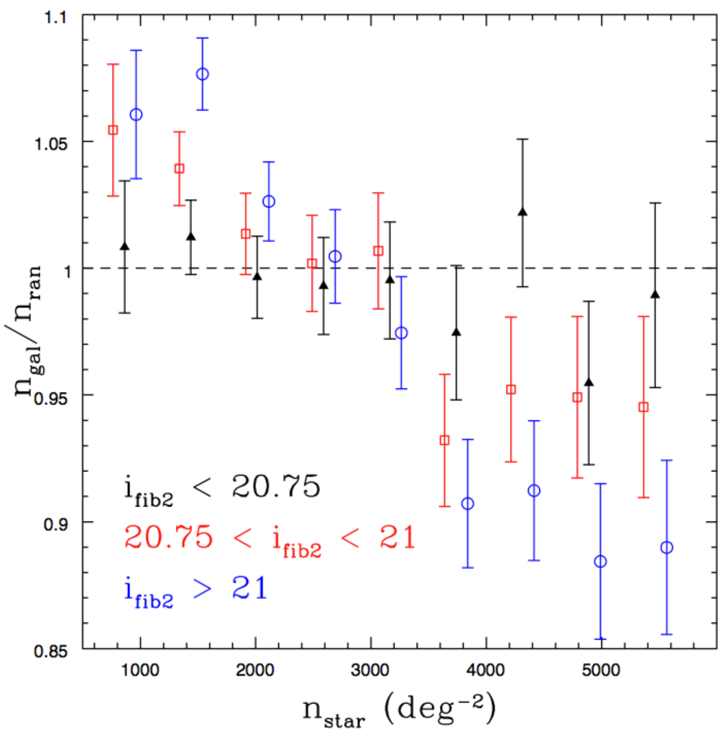

- Target density correlates with stellar density and brightness
- Corrected by weighting
- See Ross et al. for more details

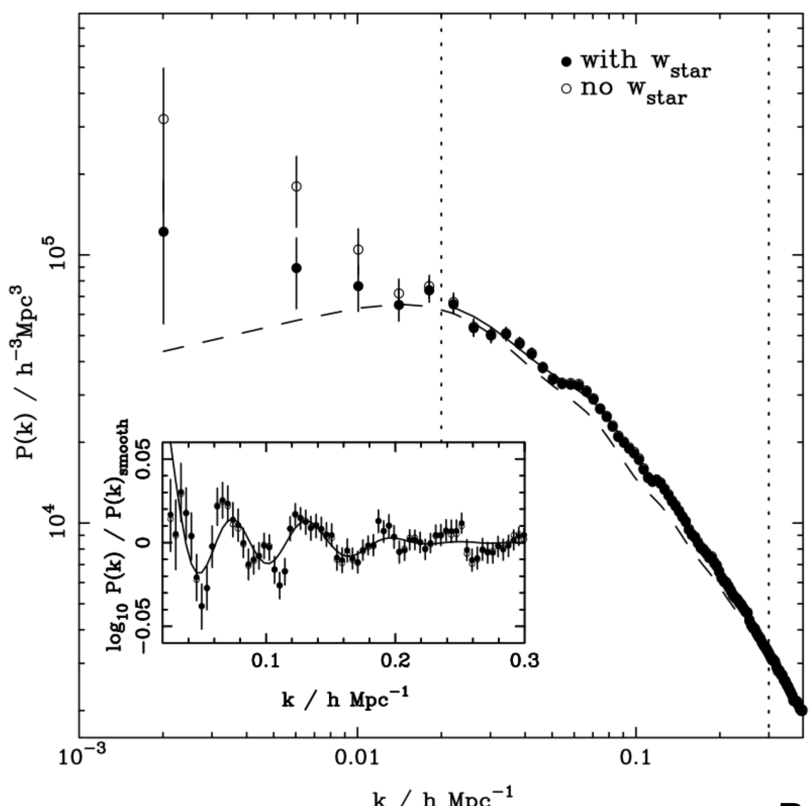

Ross et al.

Mock catalogues

- 600 mocks created by populating 2LPT field using the CMASS HOD
- Redshift-space effects added based on 2LPT velocities
- Matches simulation large-scale clustering at 10% level
- Used to test method and estimate covariances
- See Manera et al. for details

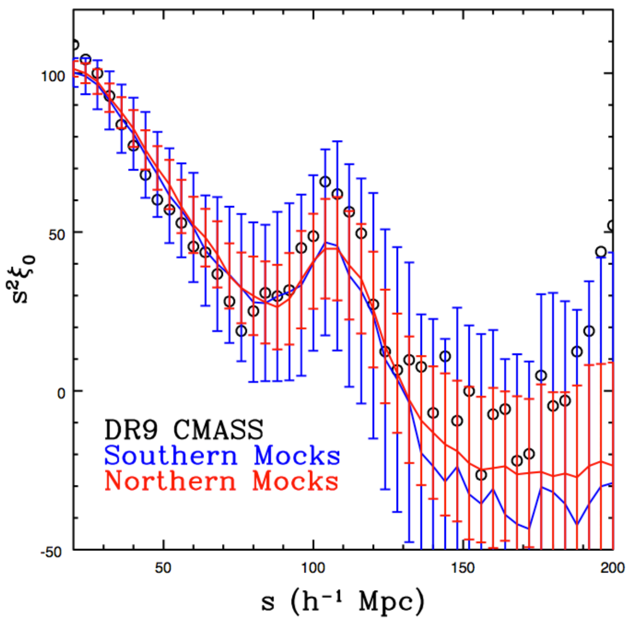

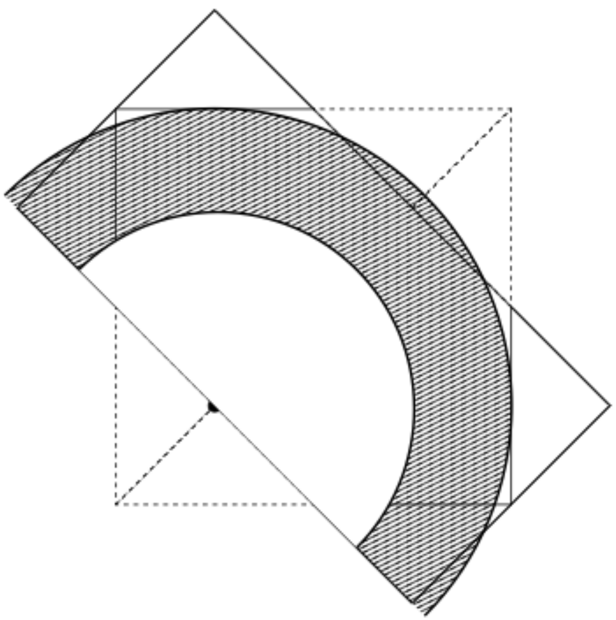

Manera et al.

Reconstruction of linear positions

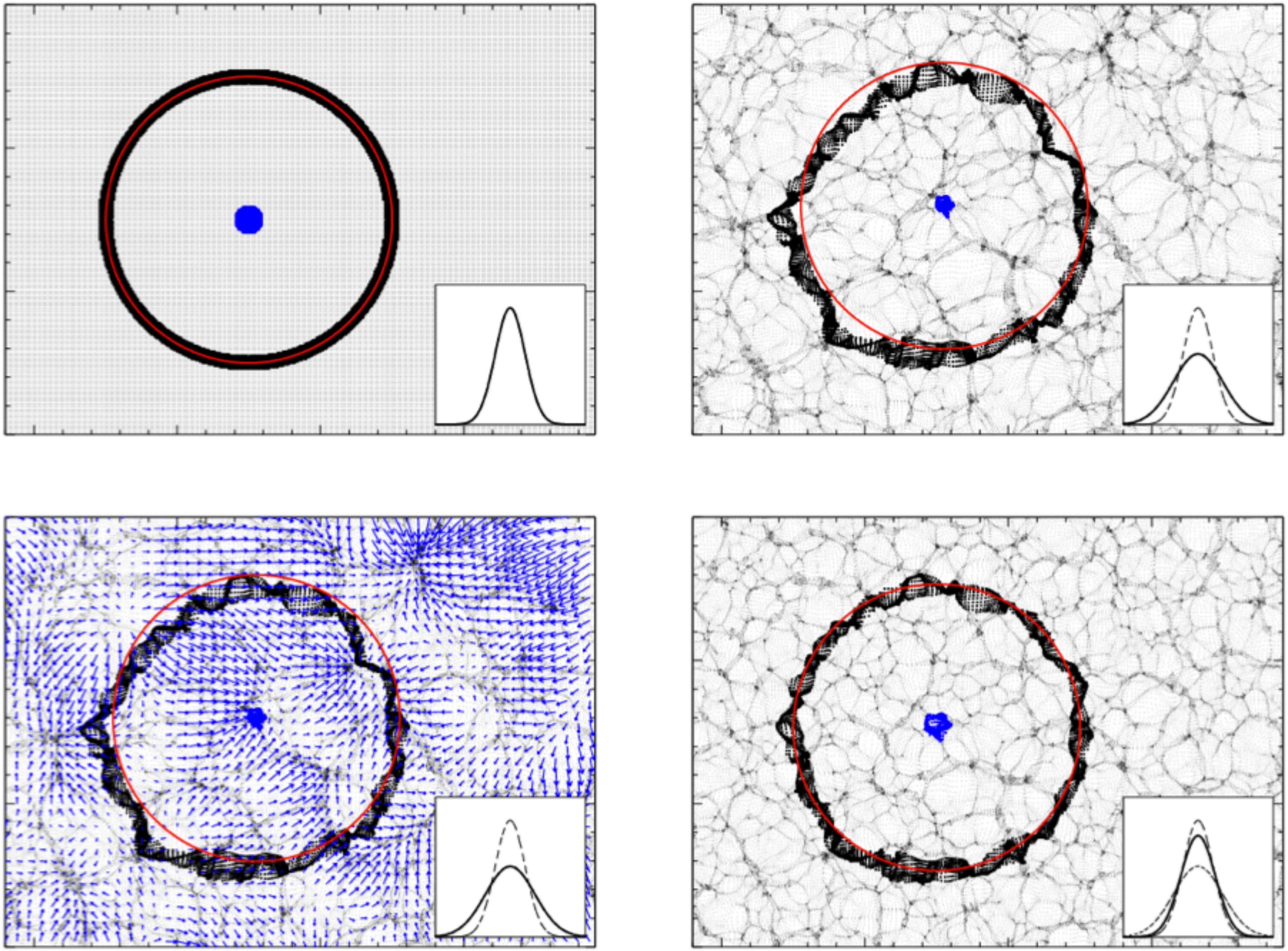

Padmanabhan et al. 2012; arXiv:1202.0090

Reconstruction on CMASS mocks

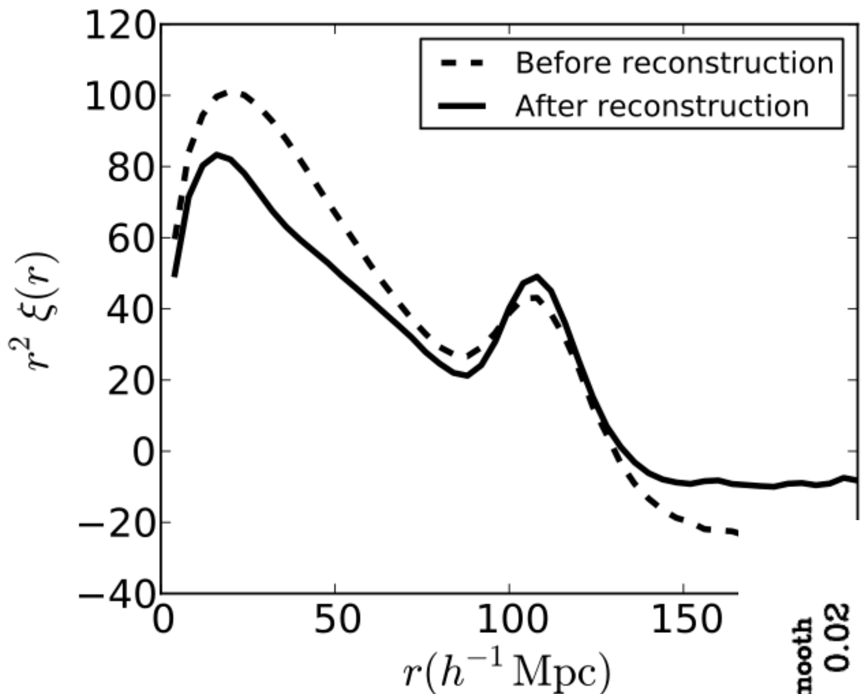

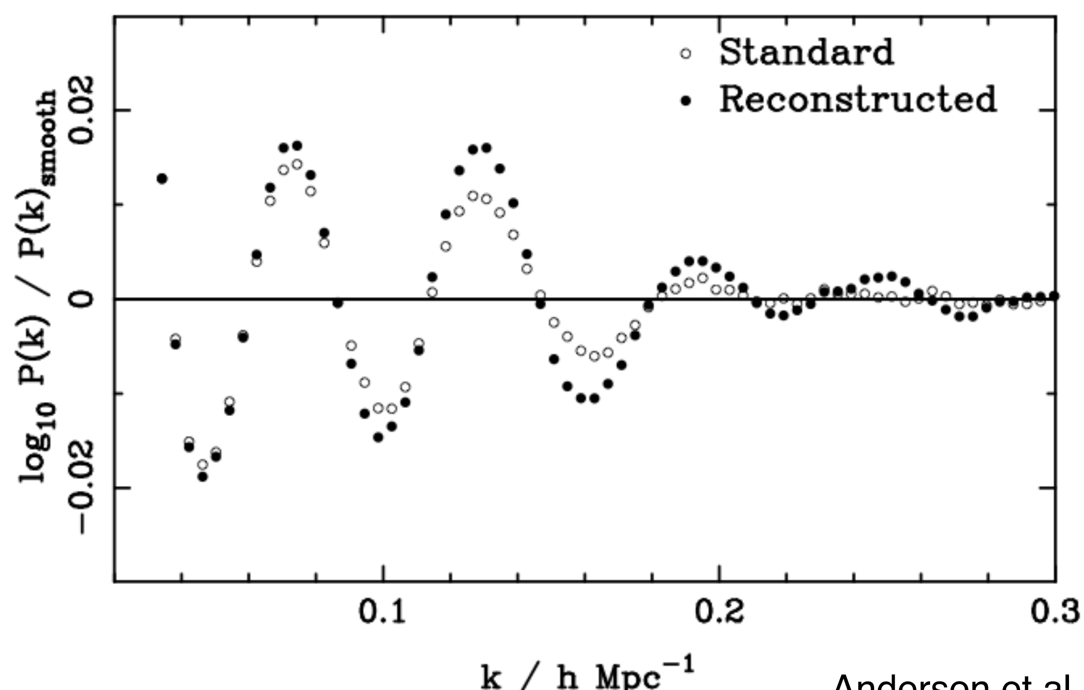

Anderson et al.

BAO results

Measuring a distance

- Fit the observed acoustic feature using some way to parametrize over nuisance broad-band features (different approaches for P(k) and ξ(r))
- Use a fiducial model to compare against observed features. Departures are quantified by a dilation scale α:

$$P(k/\alpha) \quad \xi(\alpha r)$$

- The dilation scale α depends on cosmology through:

$$D_V / r_s = \alpha (D_V / r_s)_{fid}$$

$$D_V = [cz(1 + z)^2 d_A^2 H^{-1}]^{1/3}$$

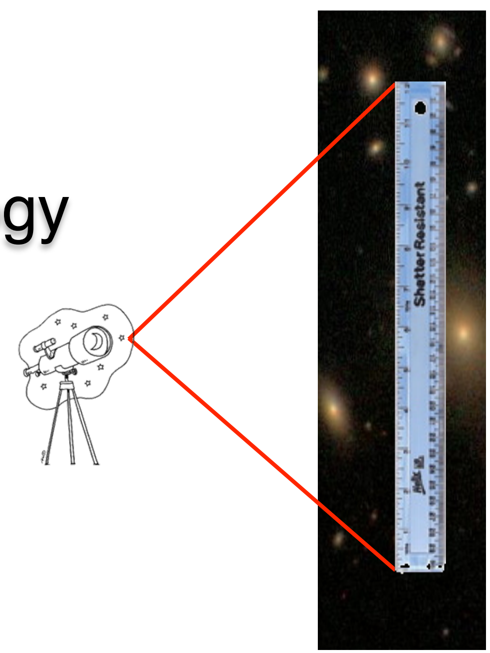

Anderson et al.

BOSS CMASS clustering measurements

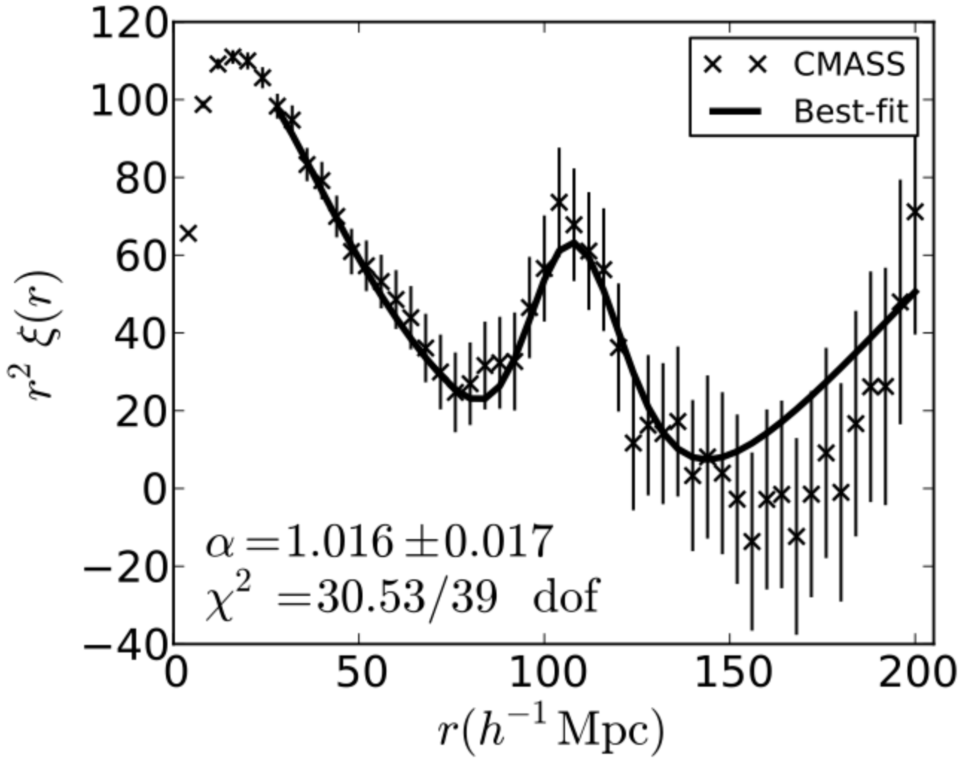

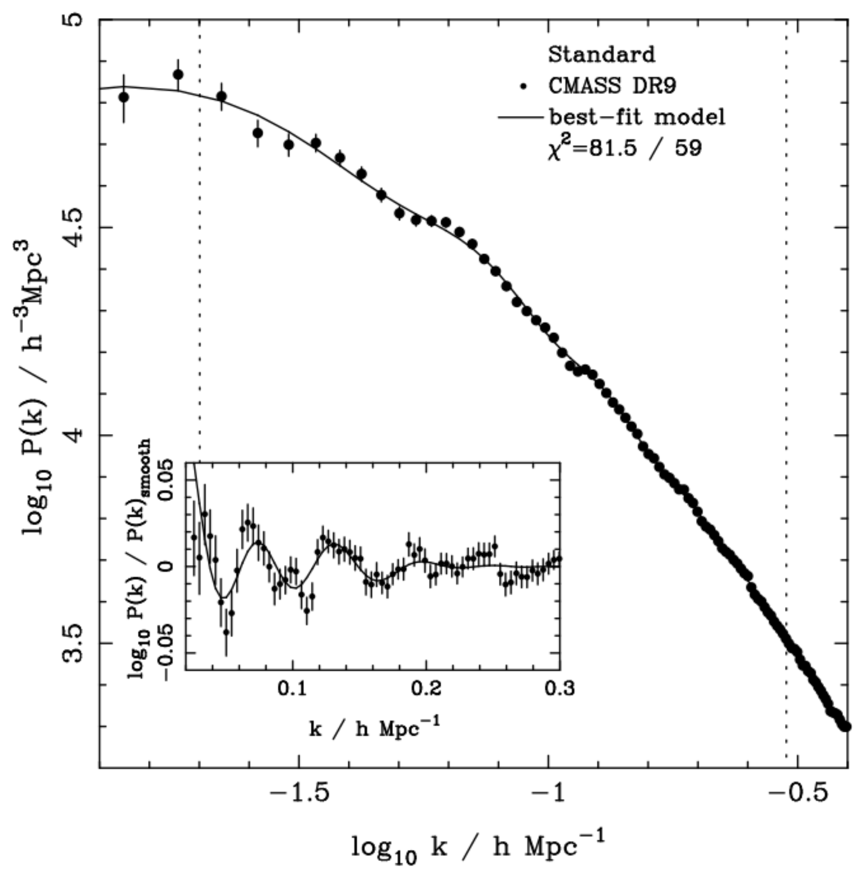

Anderson et al.

Reconstruction on CMASS

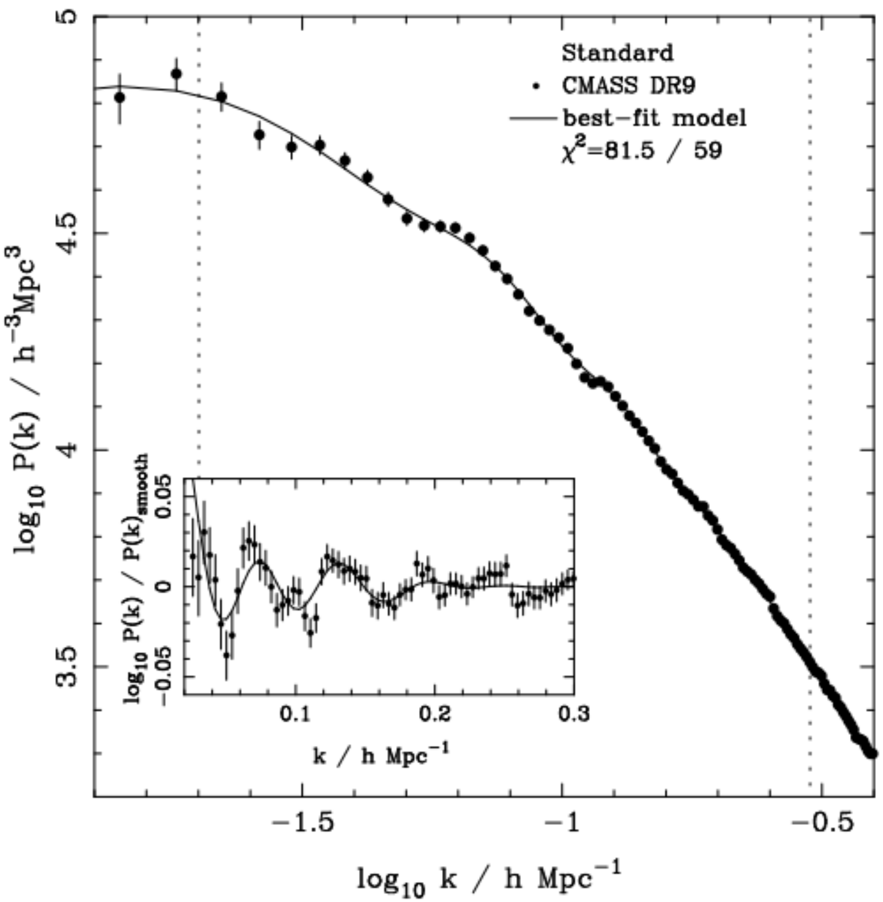

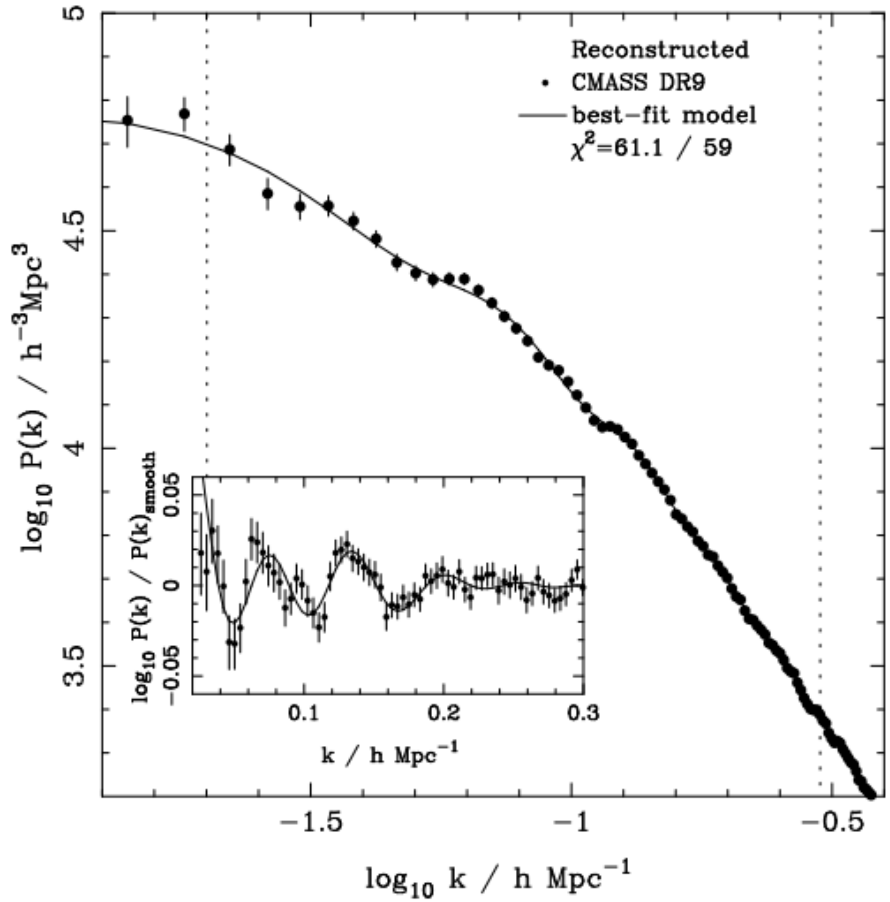

Anderson et al.

Reconstruction: error on α

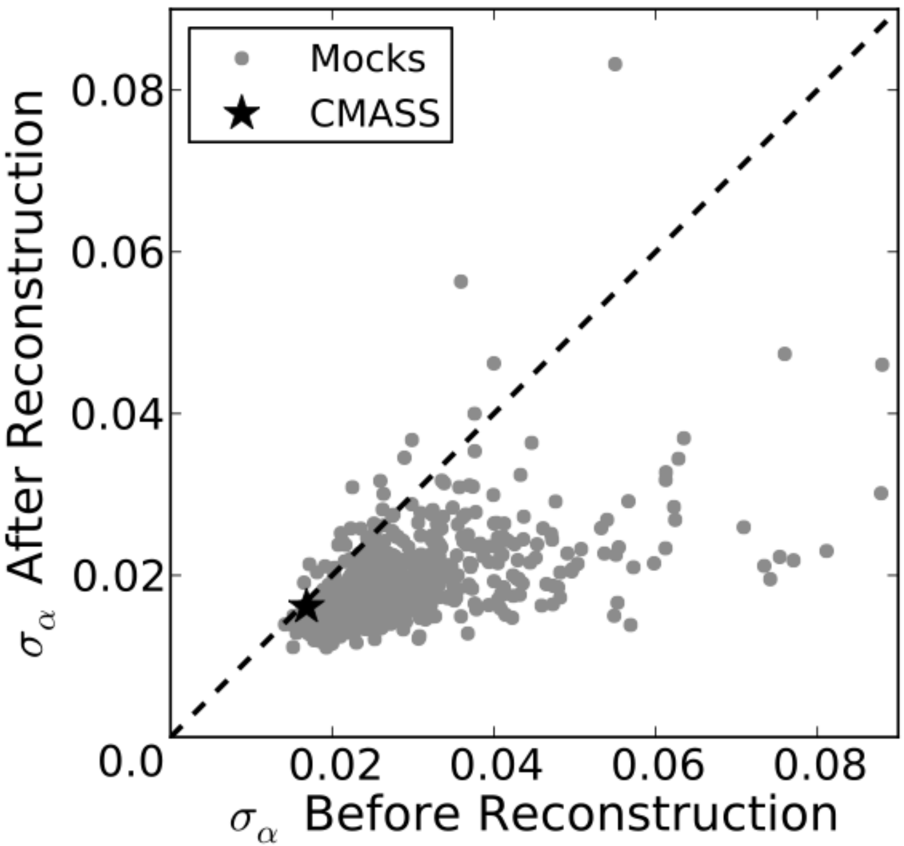

Correlation function

Power spectrum

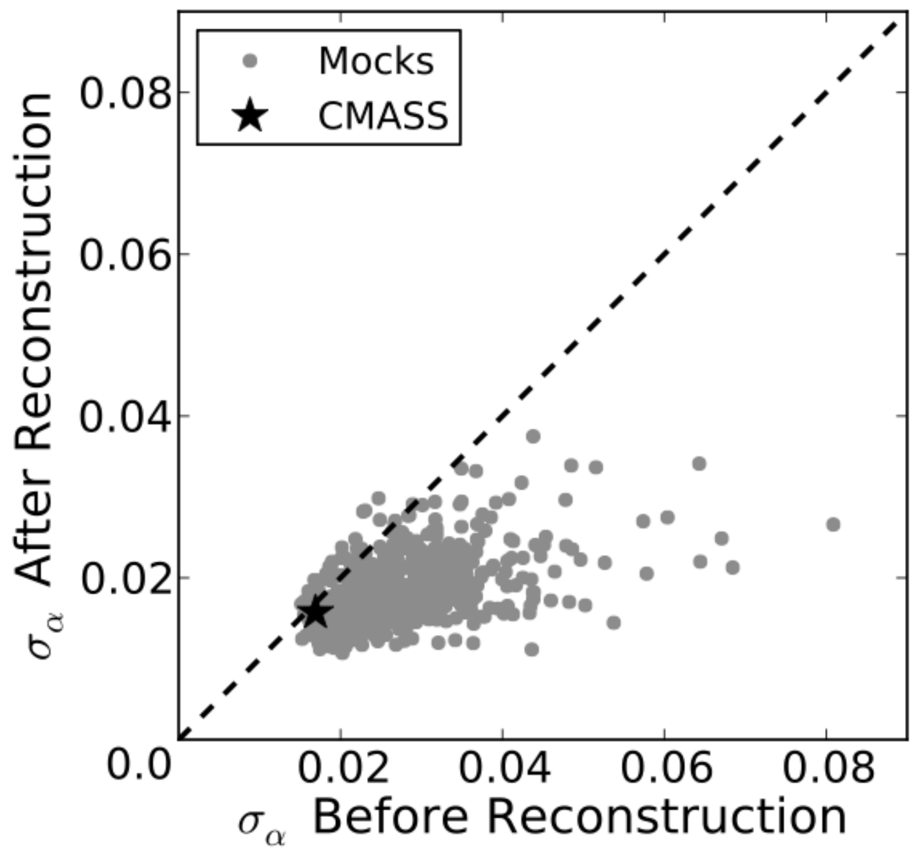

Anderson et al.

Reconstruction: α

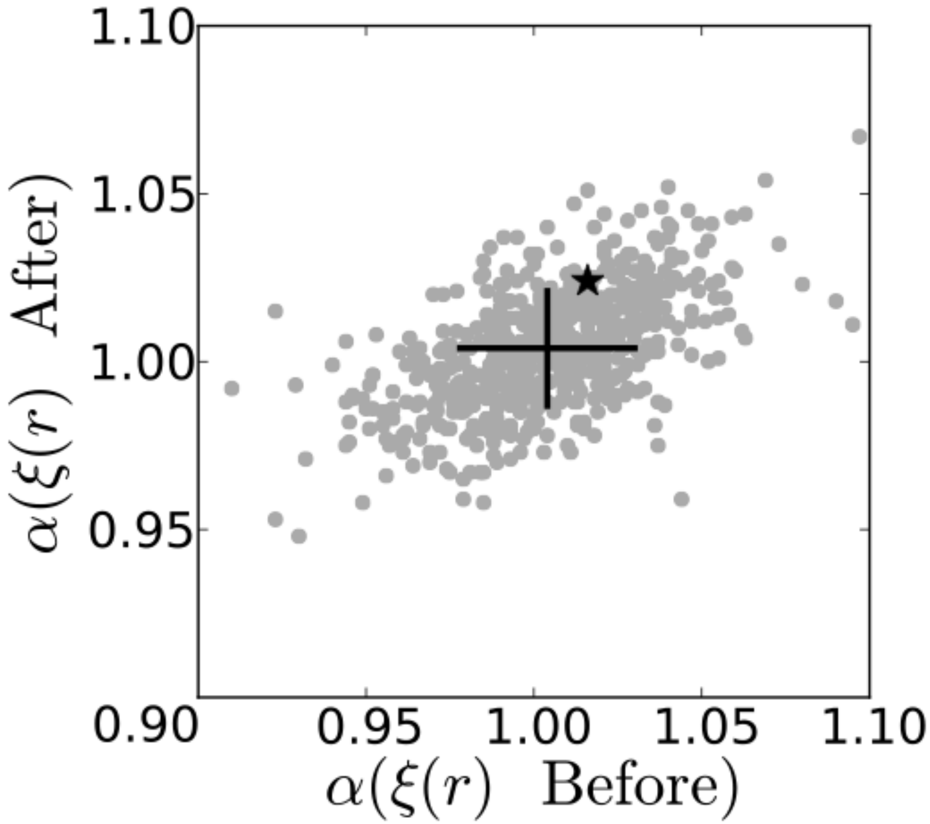

Correlation function

Power spectrum

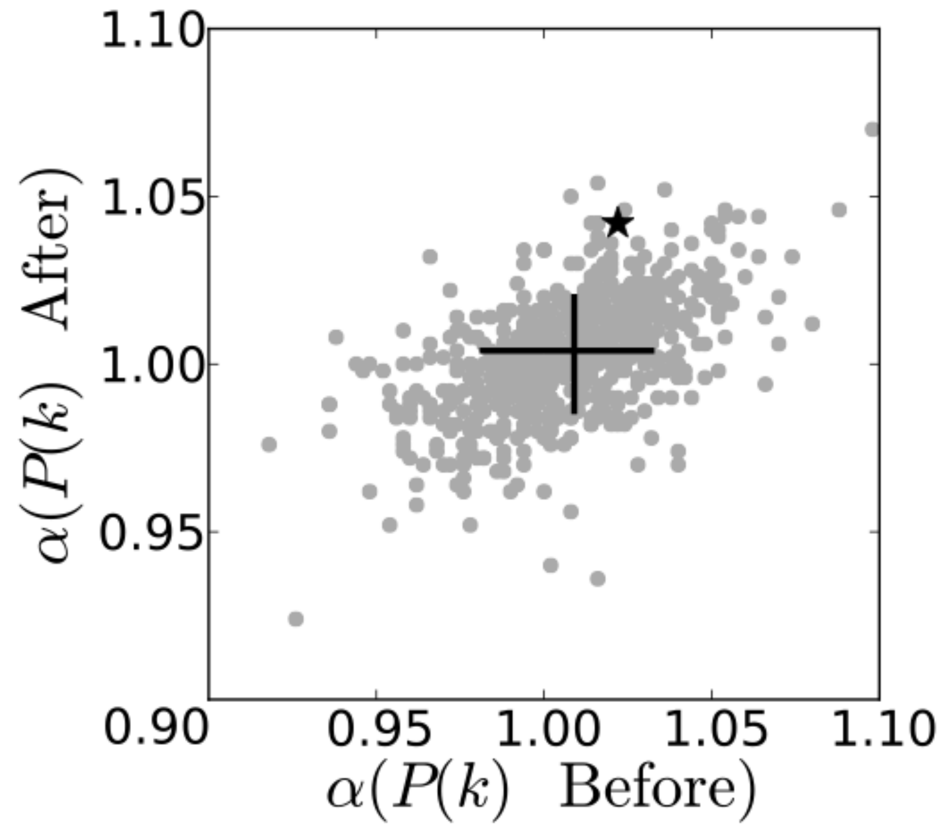

Anderson et al.

Comparison of ξ(r) & P(k) measurements

Pre-reconstruction

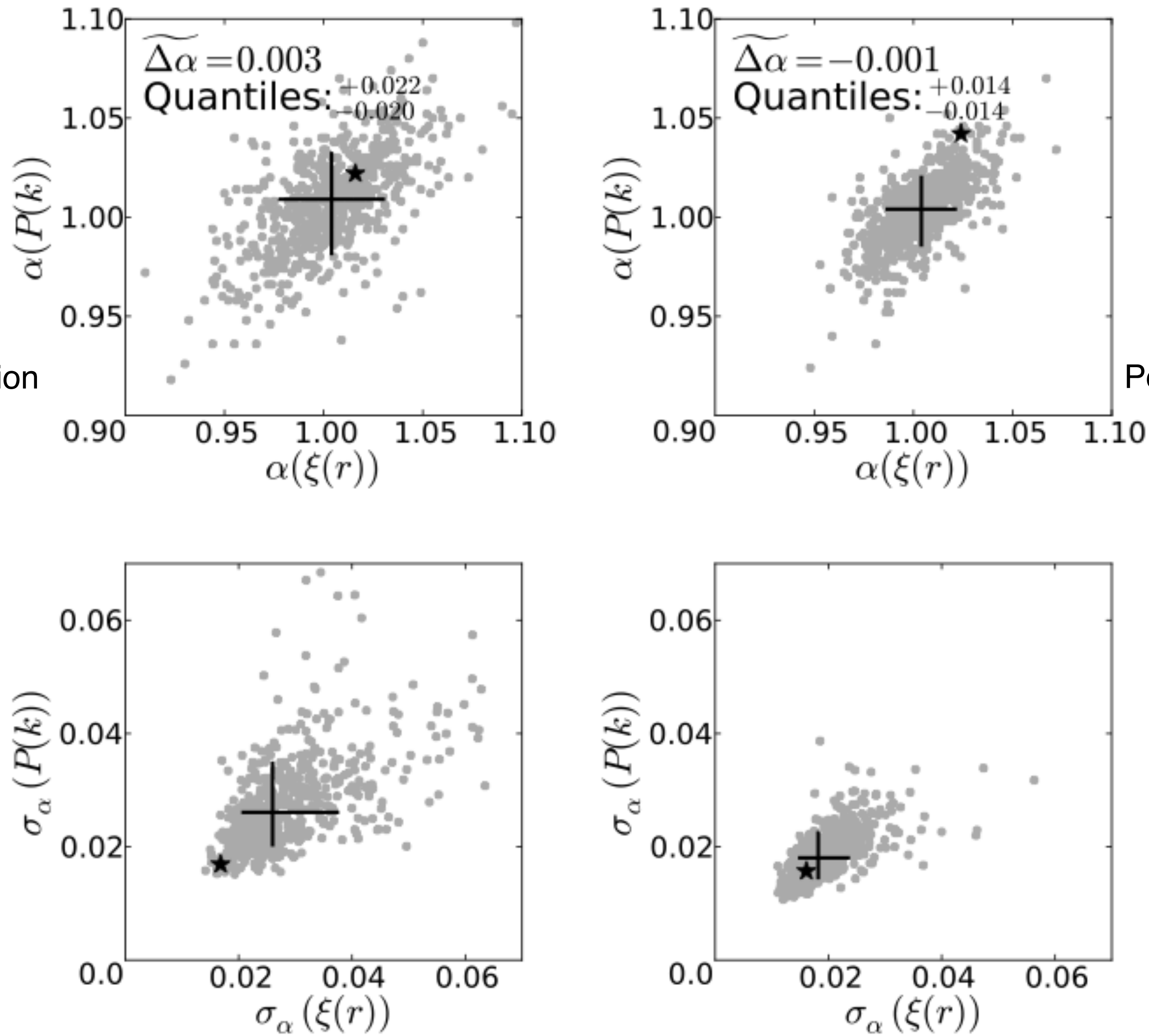

Post-reconstruction

Anderson et al.

Key BAO measurements

	α	χ^2/dof	$D_V/r_s(z=0.57)$
		Before Reconstruction	
$\xi(r)$	1.016 ± 0.017	$30.53/39$	13.44 ± 0.22
$P(k)$	1.022 ± 0.017	$81.5/59$	13.52 ± 0.22
		After Reconstruction	
$\xi(r)$	1.024 ± 0.016	$34.53/39$	13.55 ± 0.21
$P(k)$	1.042 ± 0.016	$61.1/59$	13.78 ± 0.21
Consensus	1.033 ± 0.017	$--$	13.67 ± 0.22

- ξ(r) and P(k) based estimations are **appropriate** and **unbiased,** but they include the noise from small scales and shot noise differently
- We **average** the two results, and compute the error bar using the **observed scatter** of the average value in the mocks. This shows no significant departure from a Gaussian distribution

Anderson et al.

Comparison of SDSS-II & CMASS results

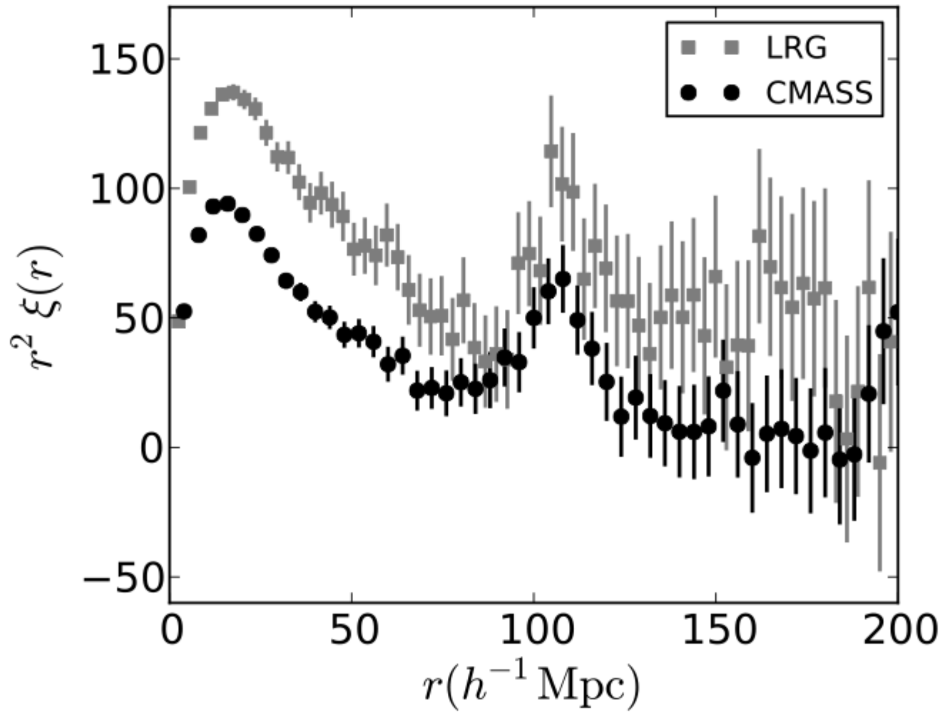

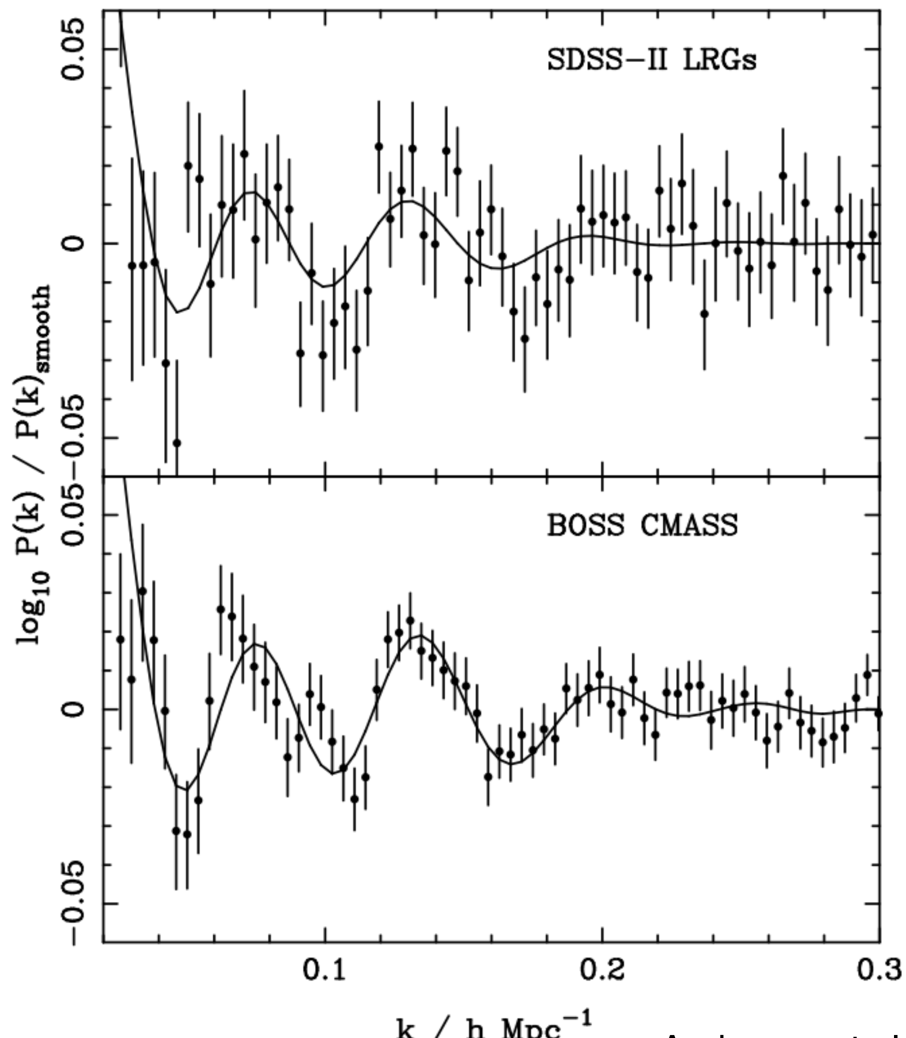

Anderson et al.

CMASS results

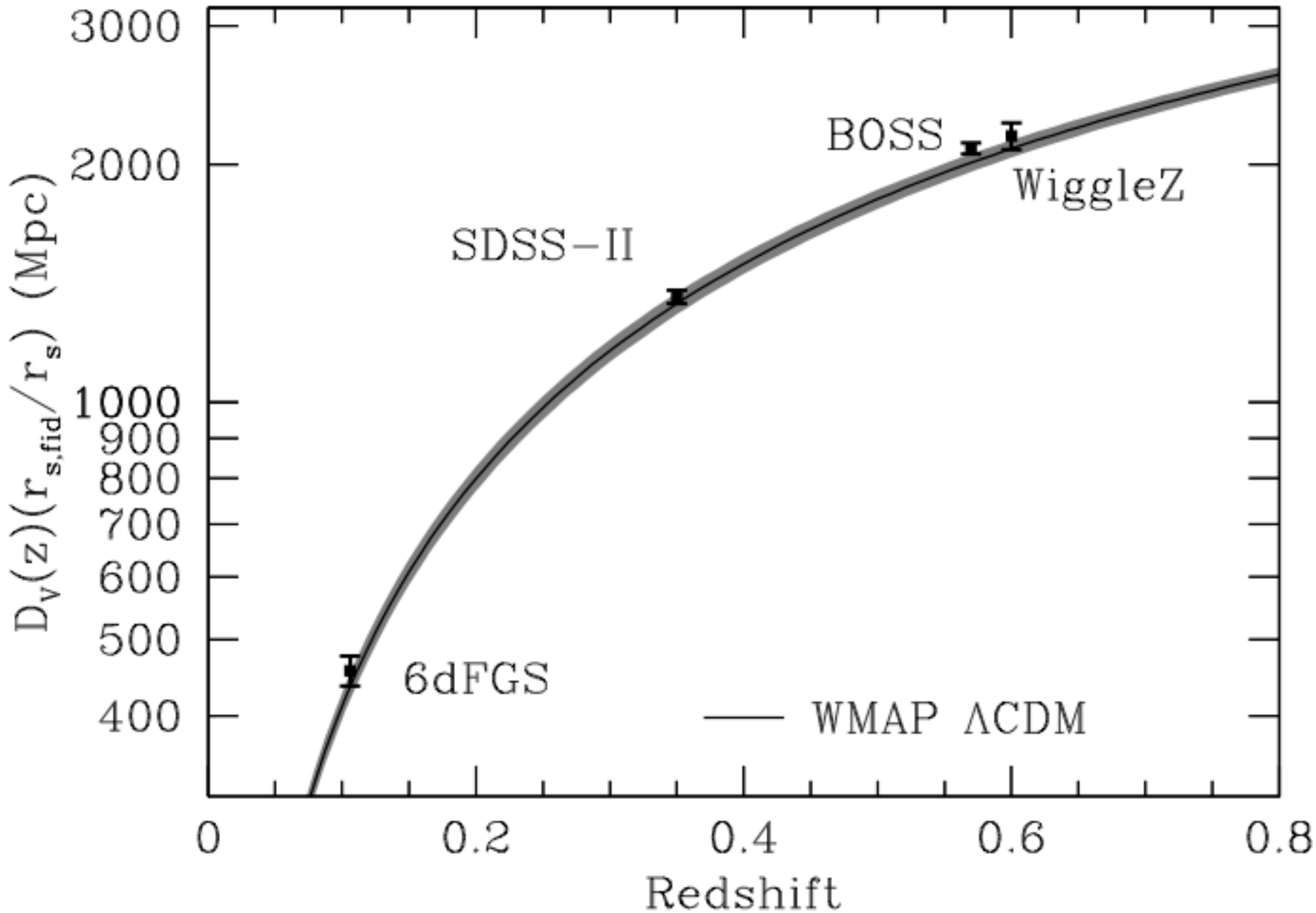

$$D_V(0.57)/r_s = 13.67 \pm 0.22$$

Anderson et al.

CMASS results

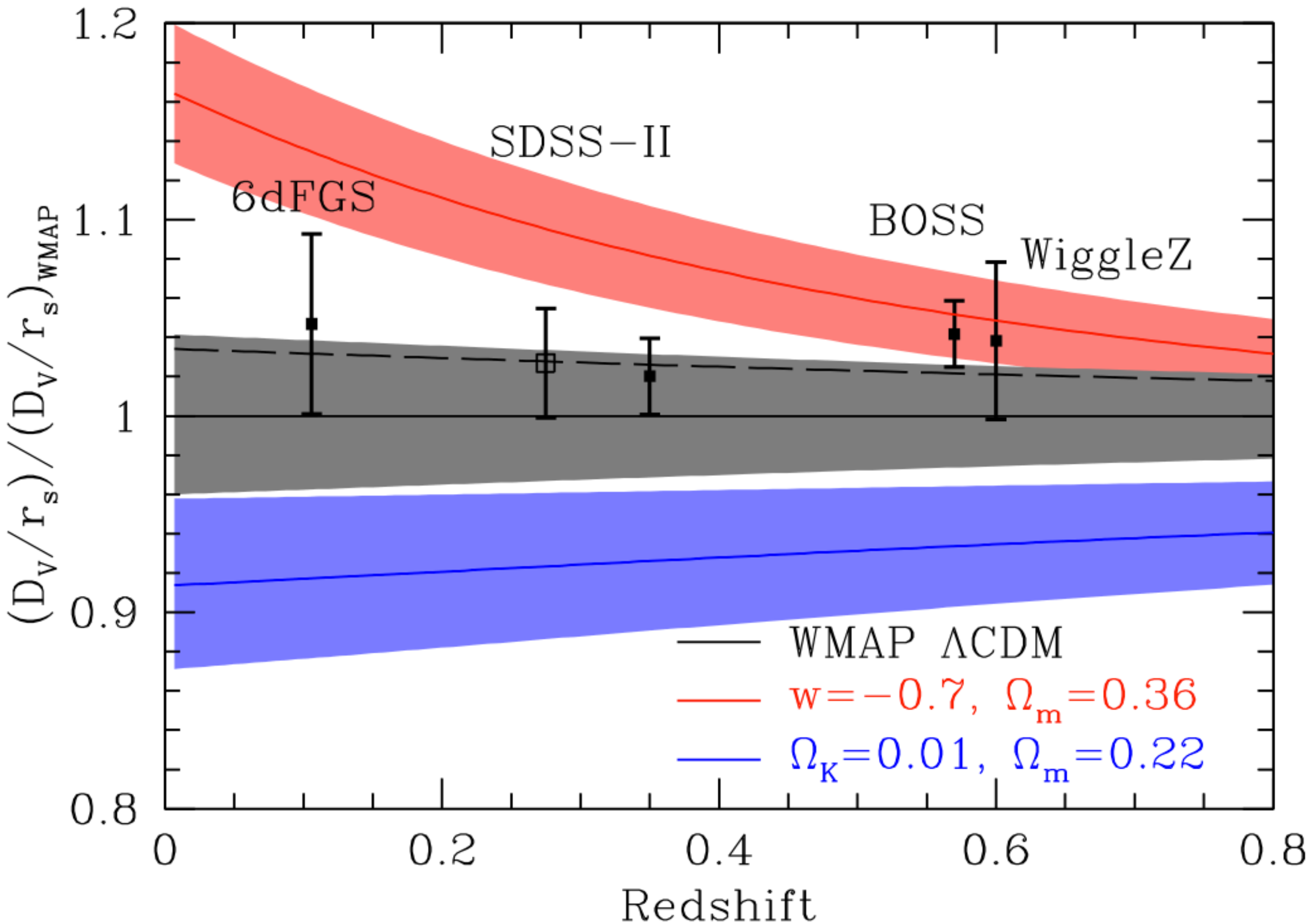

Anderson et al.

Cosmological results

Cosmological Model	Data Sets[1]	$\Omega_m h^2$	Ω_m	H_0 km/s/Mpc	Ω_K	w_0	w_a
ΛCDM	CMB	0.1341(56)	0.268(29)	71.0(26)	···	···	···
ΛCDM	CMB+CMASS	0.1392(36)	0.298(17)	68.4(13)	···	···	···
ΛCDM	CMB+LRG	0.1362(33)	0.280(14)	69.8(12)	···	···	···
ΛCDM	CMB+LRG+CMASS	0.1384(31)	0.293(12)	68.8(10)	···	···	···
ΛCDM	CMB+LRG+CMASS+6dF	0.1384(31)	0.293(12)	68.7(10)	···	···	···
ΛCDM	CMB+LRG+CMASS+SN	0.1373(30)	0.287(11)	69.2(10)	···	···	···
ΛCDM	CMB+LRG+CMASS+SN+6dF	0.1373(30)	0.288(11)	69.1(10)	···	···	···
oCDM	CMB	0.1344(55)	0.423(175)	60.0(123)	-0.039(44)	···	···
oCDM	CMB+CMASS	0.1340(53)	0.299(16)	67.0(15)	-0.008(5)	···	···
oCDM	CMB+LRG	0.1333(53)	0.278(15)	69.3(16)	-0.004(5)	···	···
oCDM	CMB+LRG+CMASS	0.1336(51)	0.288(12)	68.1(11)	-0.006(5)	···	···
oCDM	CMB+LRG+CMASS+6dF	0.1336(50)	0.288(12)	68.1(11)	-0.006(5)	···	···
oCDM	CMB+LRG+CMASS+SN	0.1322(51)	0.284(12)	68.3(12)	-0.006(5)	···	···
oCDM	CMB+LRG+CMASS+SN+6dF	0.1321(50)	0.284(12)	68.2(11)	-0.007(5)	···	···
wCDM	CMB	0.1342(58)	0.263(105)	75.4(138)	···	-1.12(41)	···
wCDM	CMB+CMASS	0.1358(59)	0.323(43)	65.4(60)	···	-0.87(24)	···
wCDM	CMB+LRG	0.1349(57)	0.285(25)	69.0(39)	···	-0.97(17)	···
wCDM	CMB+LRG+CMASS	0.1370(58)	0.294(27)	68.6(44)	···	-0.99(21)	···
wCDM	CMB+LRG+CMASS+6dF	0.1363(51)	0.298(20)	67.8(31)	···	-0.95(15)	···
wCDM	CMB+LRG+CMASS+SN	0.1399(37)	0.280(13)	70.8(18)	···	-1.09(8)	···
wCDM	CMB+LRG+CMASS+SN+6dF	0.1396(37)	0.282(13)	70.4(17)	···	-1.08(8)	···
owCDM	CMB+LRG+CMASS	0.1345(53)	0.250(42)	74.1(70)	-0.008(5)	-1.31(34)	···
owCDM	CMB+LRG+CMASS+6dF	0.1334(52)	0.271(31)	70.5(43)	-0.007(6)	-1.14(23)	···
owCDM	CMB+CMASS+SN	0.1338(53)	0.280(17)	69.2(21)	-0.009(5)	-1.10(8)	···
owCDM	CMB+LRG+CMASS+SN	0.1337(53)	0.275(14)	69.8(18)	-0.007(5)	-1.09(8)	···
owCDM	CMB+LRG+CMASS+SN+6dF	0.1333(52)	0.276(13)	69.6(17)	-0.008(5)	-1.09(8)	···
$w_0 w_a$CDM	CMB+LRG+CMASS	0.1377(58)	0.282(52)	70.7(68)	···	-1.11(51)	0.18(122)*
$w_0 w_a$CDM	CMB+LRG+CMASS+6dF	0.1369(55)	0.292(41)	68.9(48)	···	-1.02(42)	0.44(113)*
$w_0 w_a$CDM	CMB+CMASS+SN	0.1389(62)	0.281(17)	70.3(23)	···	-1.07(16)	-0.85(96)*
$w_0 w_a$CDM	CMB+LRG+CMASS+SN	0.1392(59)	0.280(14)	70.6(19)	···	-1.08(15)	0.10(87)
$w_0 w_a$CDM	CMB+LRG+CMASS+SN+6dF	0.1385(58)	0.281(14)	70.2(17)	···	-1.08(15)	0.08(81)
o$w_0 w_a$CDM	CMB+LRG+CMASS	0.1347(54)	0.263(54)	72.7(79)	-0.009(6)	-1.13(54)	-0.70(139)*
o$w_0 w_a$CDM	CMB+LRG+CMASS+6dF	0.1341(53)	0.284(40)	69.2(50)	-0.009(7)	-0.93(41)	-0.93(130)*
o$w_0 w_a$CDM	CMB+CMASS+SN	0.1344(54)	0.280(17)	69.5(21)	-0.012(6)	-0.91(17)	-1.31(102)*
o$w_0 w_a$CDM	CMB+LRG+CMASS+SN	0.1348(53)	0.277(14)	69.8(18)	-0.012(5)	-0.89(16)	-1.44(93)*
o$w_0 w_a$CDM	CMB+LRG+CMASS+SN+6dF	0.1343(52)	0.278(14)	69.5(17)	-0.012(5)	-0.88(15)	-1.40(94)*
o$w_0 w_a$CDM	CMB+LRG+CMASS+SN+H0	0.1364(51)	0.270(12)	71.1(15)	-0.010(5)	-0.93(16)	-1.46(95)*
o$w_0 w_a$CDM	CMB+LRG+CMASS+SN+H0+6dF	0.1359(50)	0.270(12)	70.8(14)	-0.010(5)	-0.93(16)	-1.39(96)*

Anderson et al.

Constraints on Friedman equation

$$H^2(a) = H_0^2 \Big[\Omega_R a^{-4} + \Omega_M a^{-3} + \Omega_k a^{-2} + \Omega_{DE} \exp \left\{ 3 \int_a^1 \frac{da'}{a'} \left[1 + w(a') \right] \right\} \Big]$$

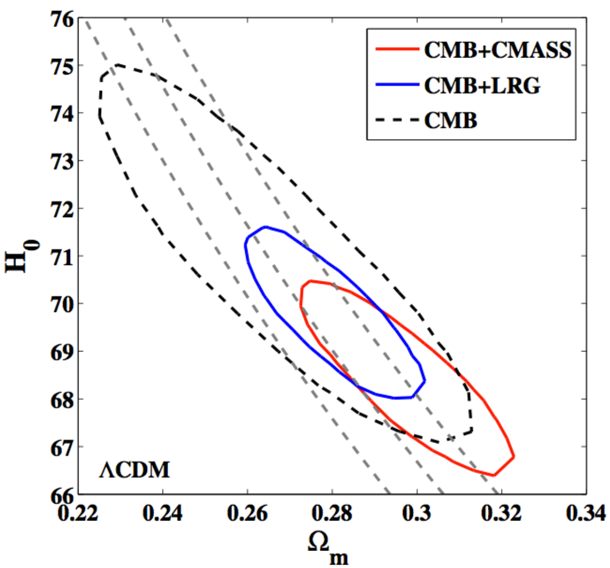

2-param ΛCDM model

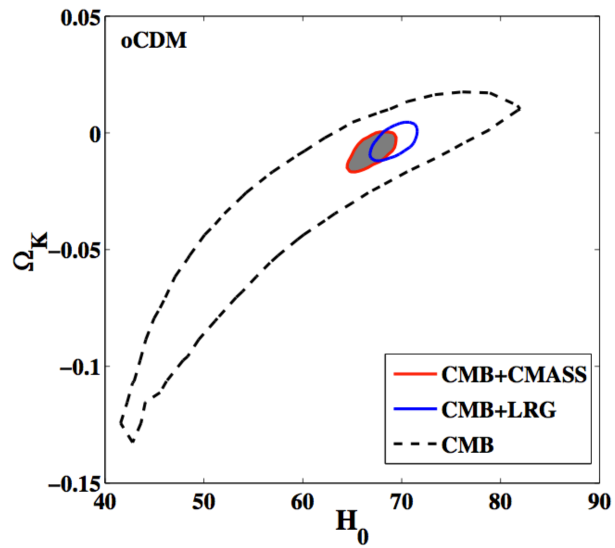

3-param oCDM model

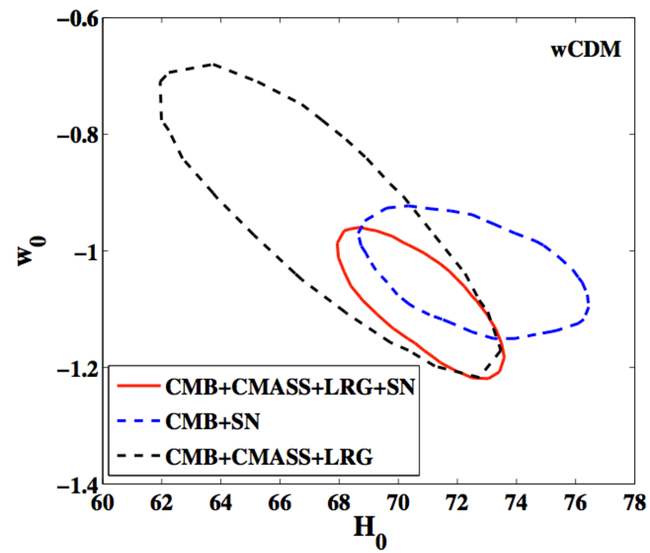

4-param wCDM model

Anderson et al.

Anisotropic clustering results

Anisotropic clustering measurements

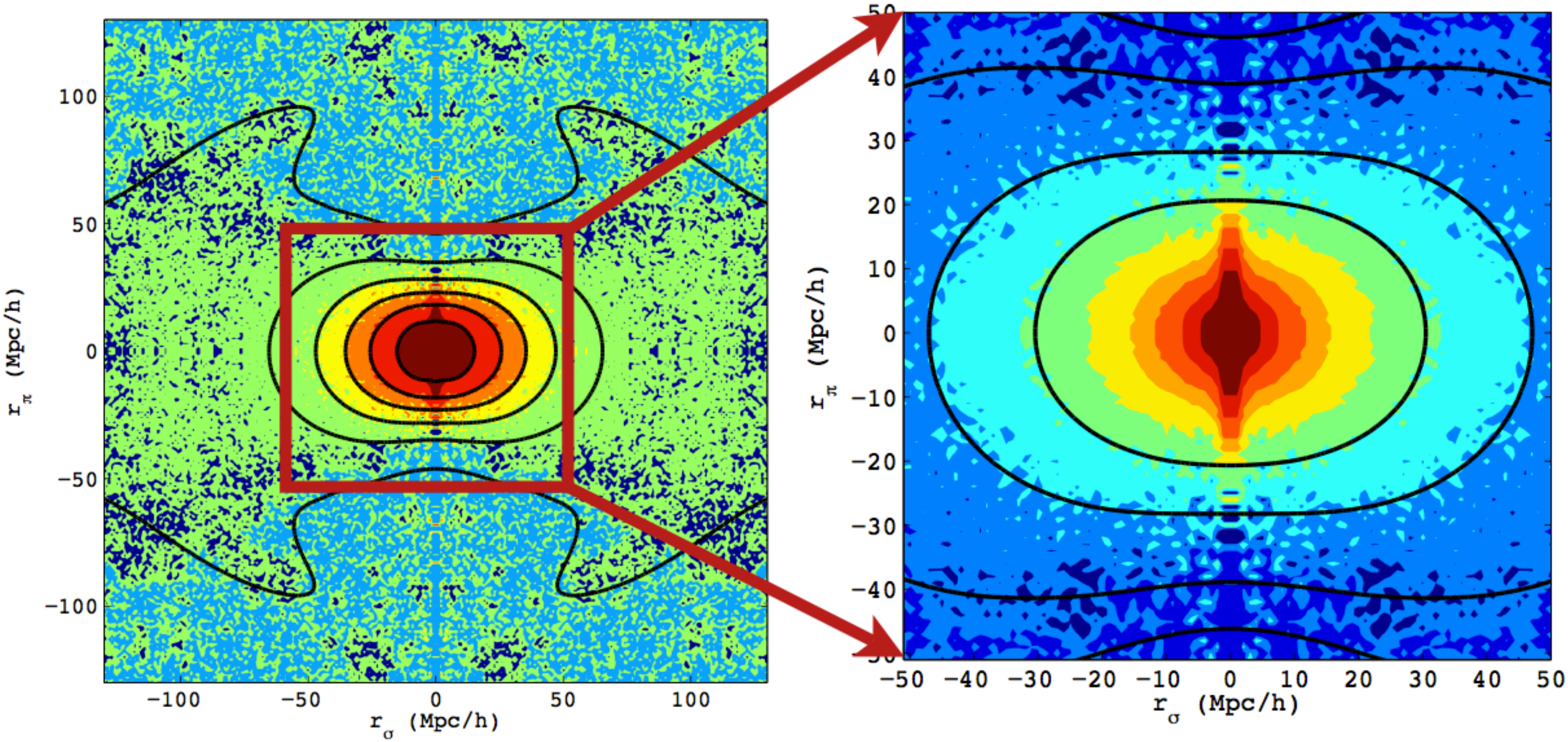

Reid et al.

Extra information from anisotropic measurements

- Including the quadrupole allows us to measure H and d_A separately (or include an additional measurement of F)

$$F = (1+z)\, d_A(z) H(z)/c$$

- F is sometimes called the Alcock-Paczynski parameter
- Can also measure the growth rate from the RSD contribution

$$f\sigma_8(z=0.57)$$

- These are degenerate, but that degeneracy is not perfect

Reid et al.

Measuring F & $f\sigma_8$

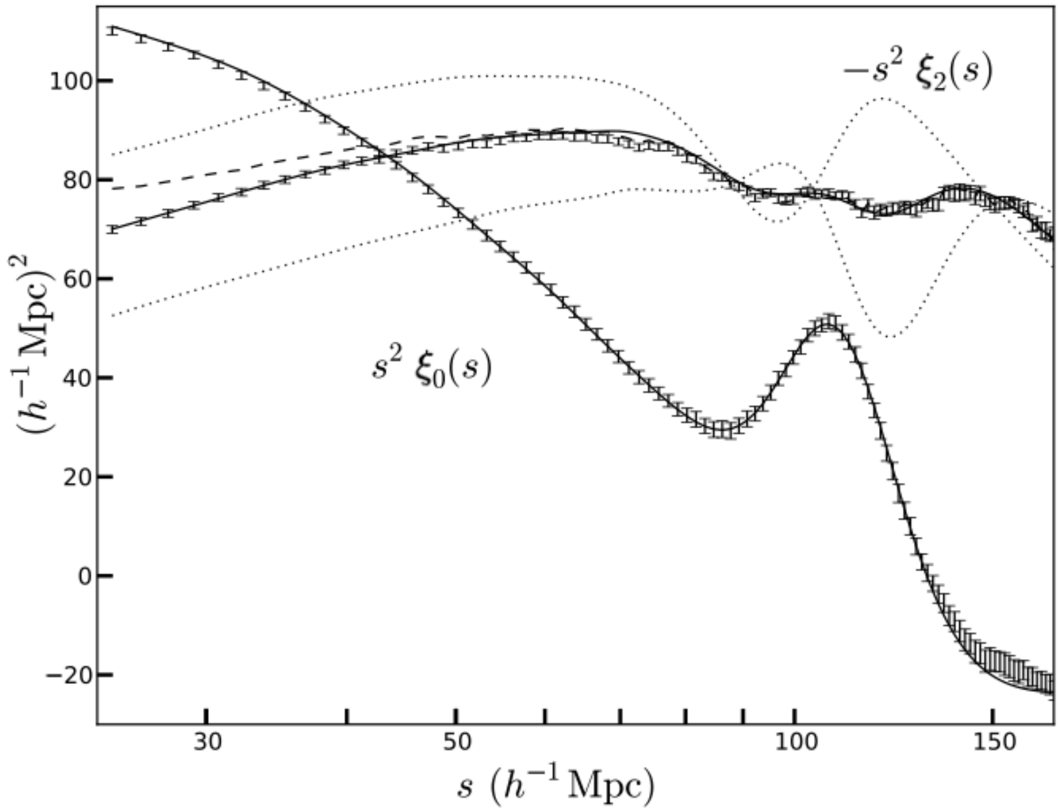

Varying F by 10%, while keeping D_V fixed

Scale-dependence of F variations allows measurements of F & $f\sigma_8$ to be separated

Reid et al.

Results of the anisotropic fit

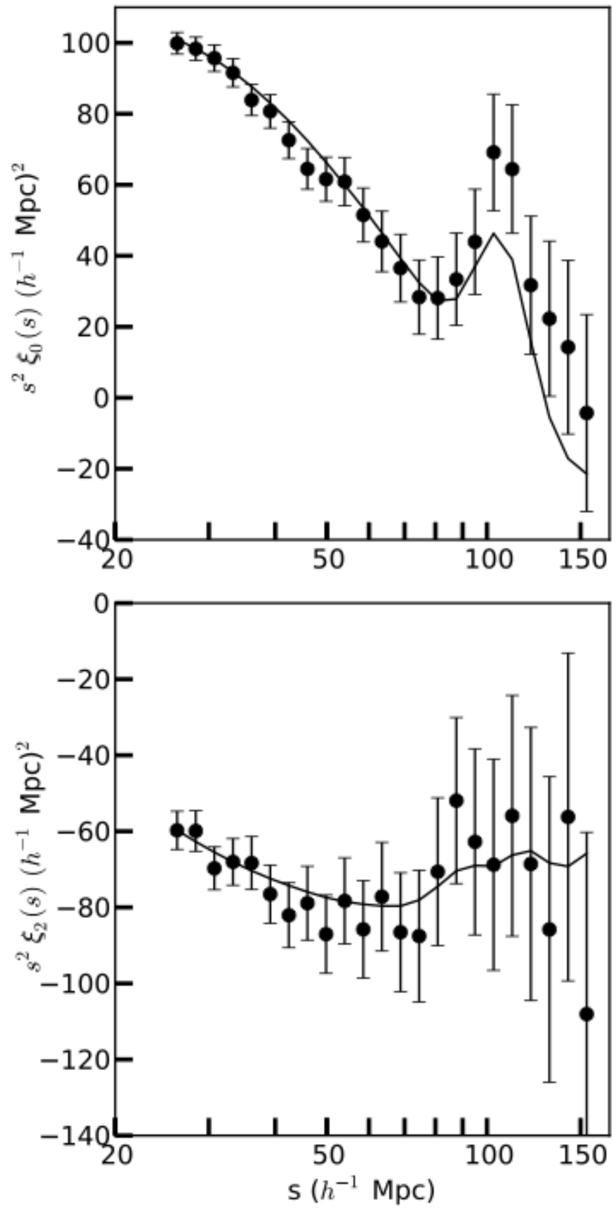

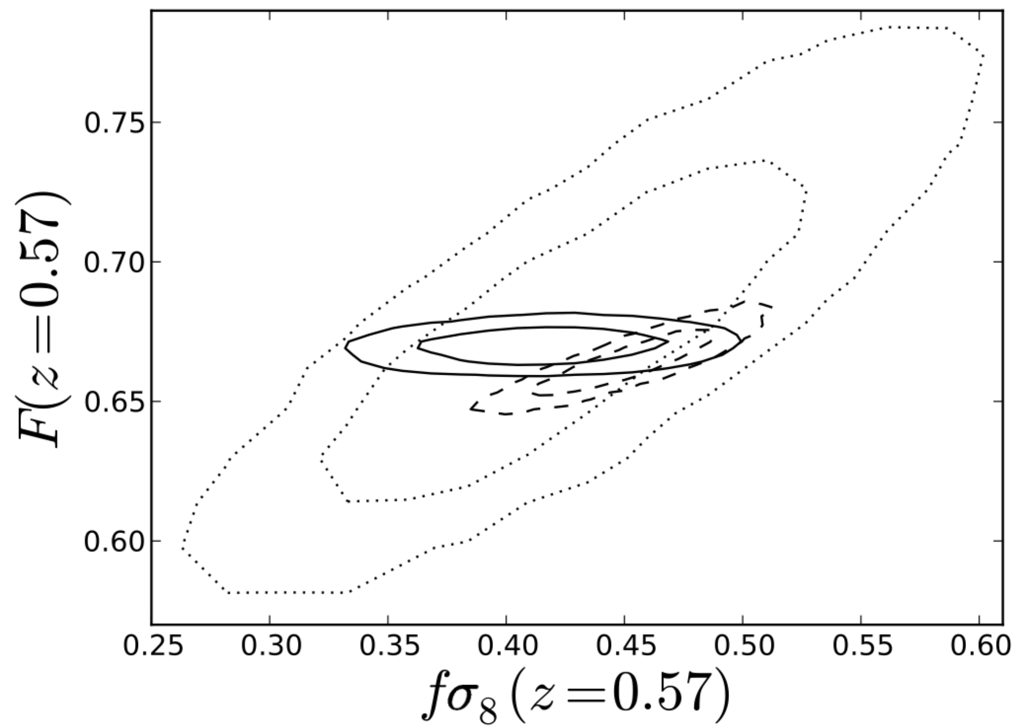

Dotted: free growth, geometry, ΛCDM prior on large-scale linear P(k) shape at z=0.57

Solid: F forced to match ΛCDM model

Dashed: WMAP ΛCDM+GR prediction

Reid et al.

CMASS F measurements in context

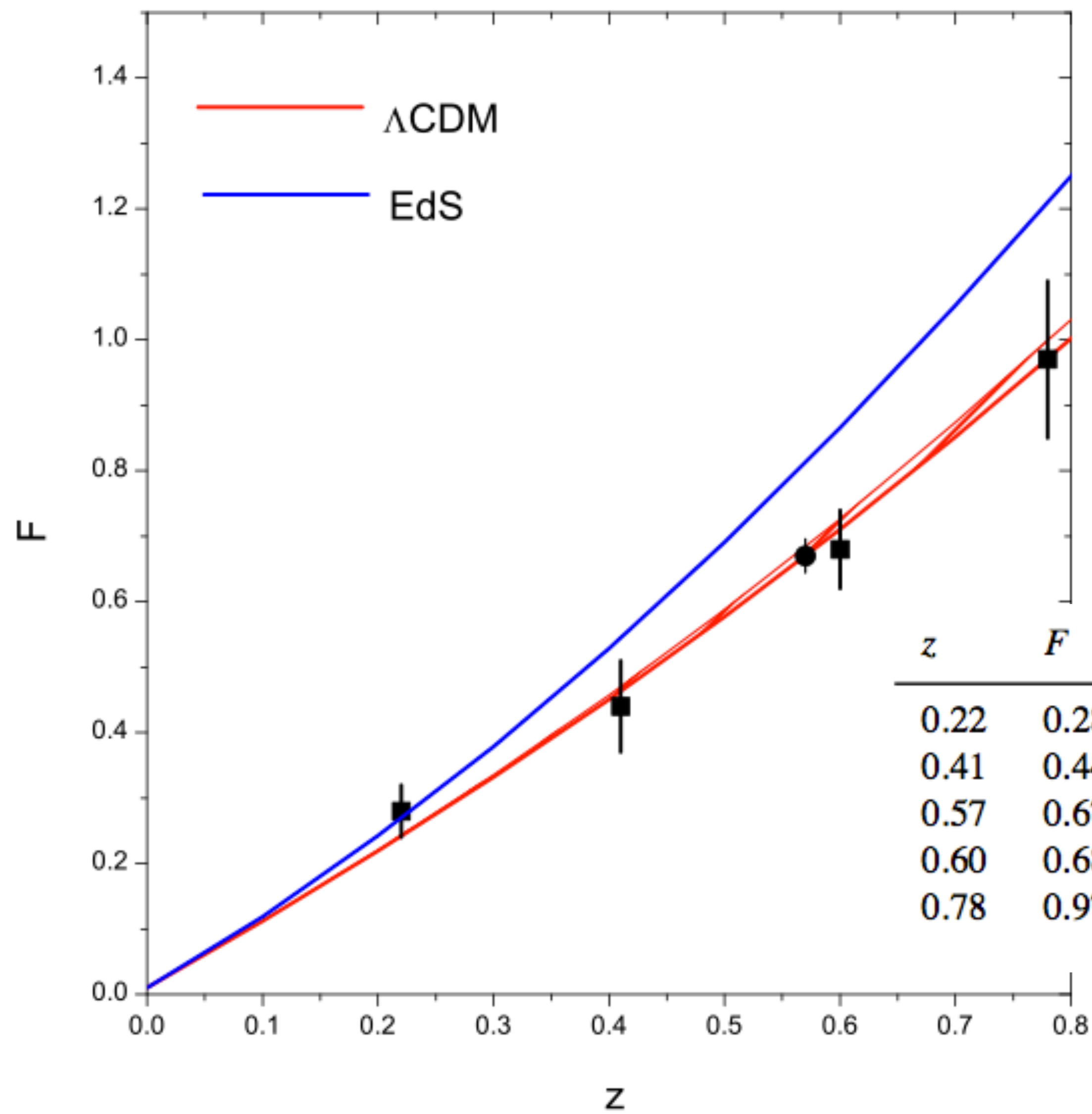

z	F	survey	reference
0.22	0.28 ± 0.04	WiggleZ	Blake, et al. (2011c)
0.41	0.44 ± 0.07	WiggleZ	Blake, et al. (2011c)
0.57	0.67 ± 0.026	BOSS	Reid et al. (2012)
0.60	0.68 ± 0.06	WiggleZ	Blake, et al. (2011c)
0.78	0.97 ± 0.12	WiggleZ	Blake, et al. (2011c)

Samushia et al. (in prep), Reid et al.

CMASS RSD measurements in context

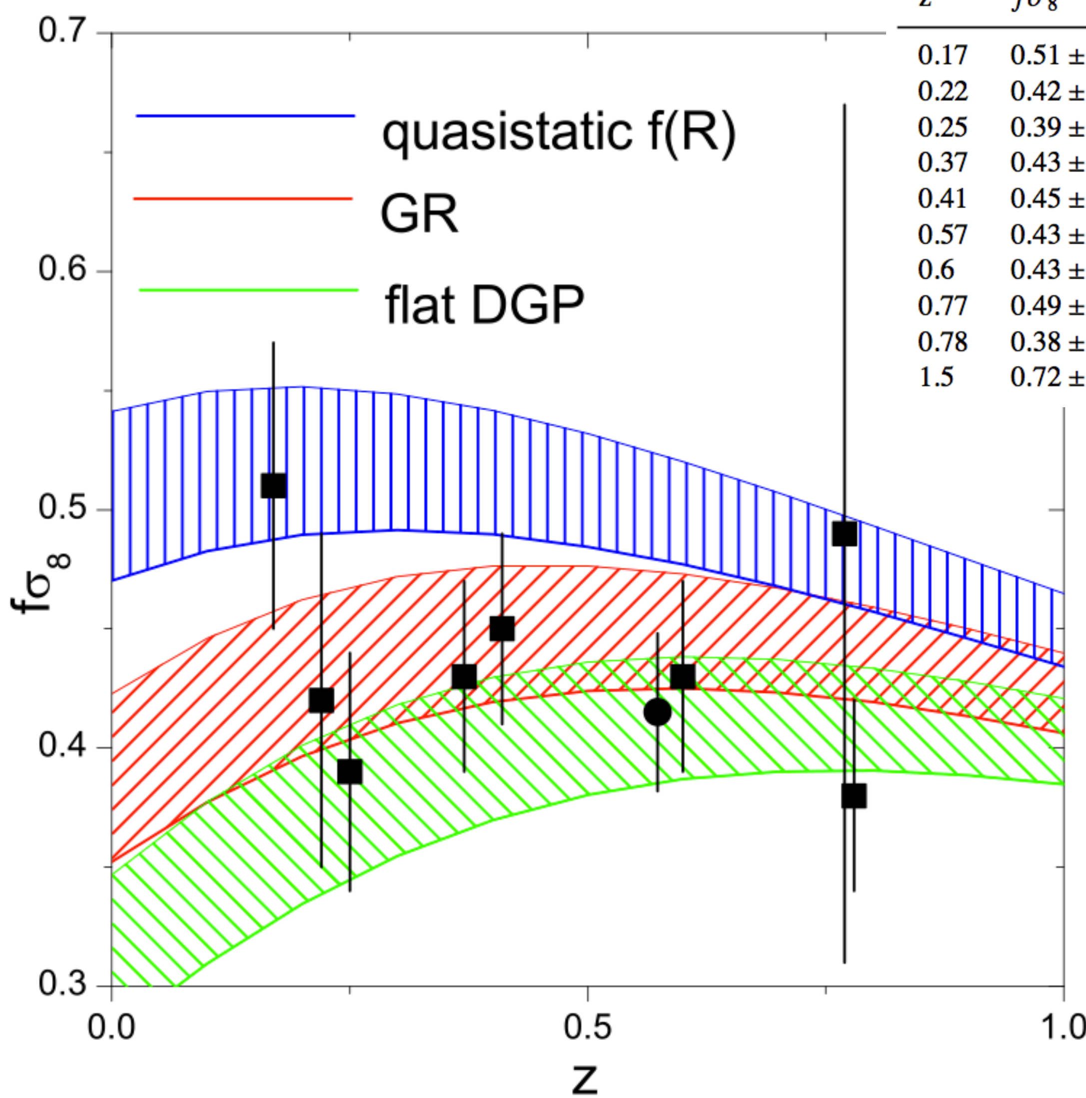

z	$f\sigma_8$	survey	reference
0.17	0.51 ± 0.06	2dFGRS	Percival et al. (2004)
0.22	0.42 ± 0.07	WiggleZ	Blake, et al. (2011b)
0.25	0.39 ± 0.05	SDSS	Samushia, Percival, & Raccanelli (2011)
0.37	0.43 ± 0.04	SDSS	Samushia, Percival, & Raccanelli (2011)
0.41	0.45 ± 0.04	WiggleZ	Blake, et al. (2011b)
0.57	0.43 ± 0.03	BOSS	Reid et al. (2012)
0.6	0.43 ± 0.04	WiggleZ	Blake, et al. (2011b)
0.77	0.49 ± 0.18	VVDS	Guzzo et al. (2007)
0.78	0.38 ± 0.04	WiggleZ	Blake, et al. (2011b)
1.5	0.72 ± 0.15	2SLAQ	da Angela et al. (2008)

Samushia et al. (in prep), Reid et al.

Using passive evolution to enhance RSD measurements

Most luminous 40% of CMASS sample are direct and passive progenitors of the SDSS-II LRG sample to within ~2%

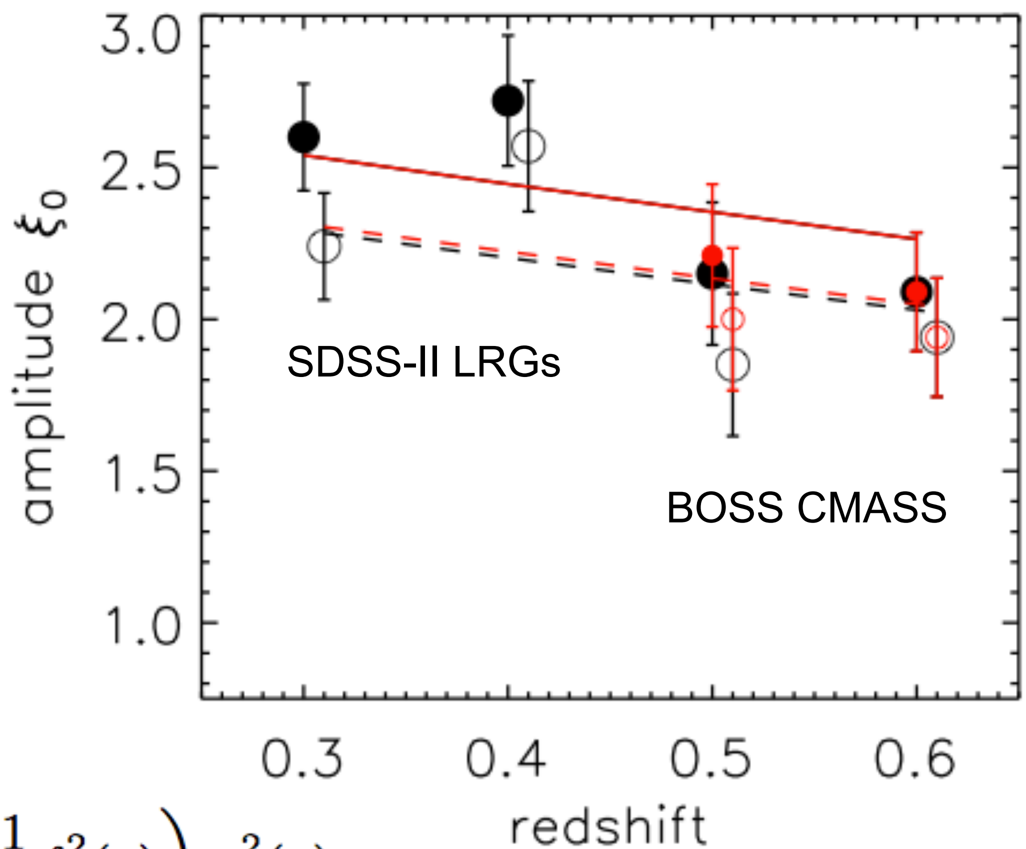

Line shows Fry (1996) model for a passively evolving population

$$A_0(z) = \left(b^2(z) + \frac{2}{3}f(z)b(z) + \frac{1}{5}f^2(z)\right)\sigma_8^2(z)$$

$$b(z) = [b(z_0) - 1]\frac{D(0)}{D(z_0)} + 1$$

Tojeiro et al. 2012; arXiv:1202.6241

Using passive evolution to enhance RSD measurements

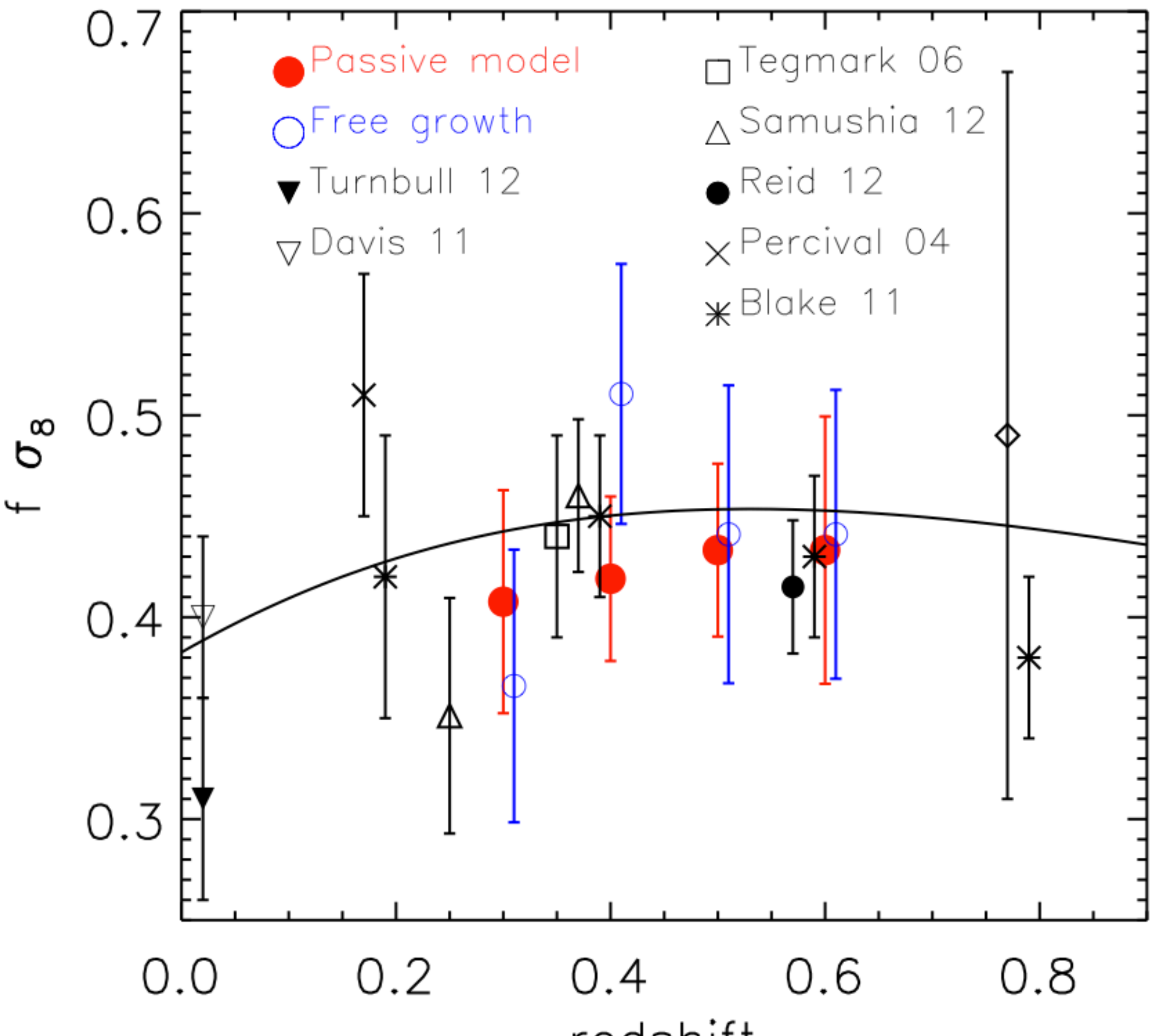

Tojeiro et al.

Converting to σ_8 measurements

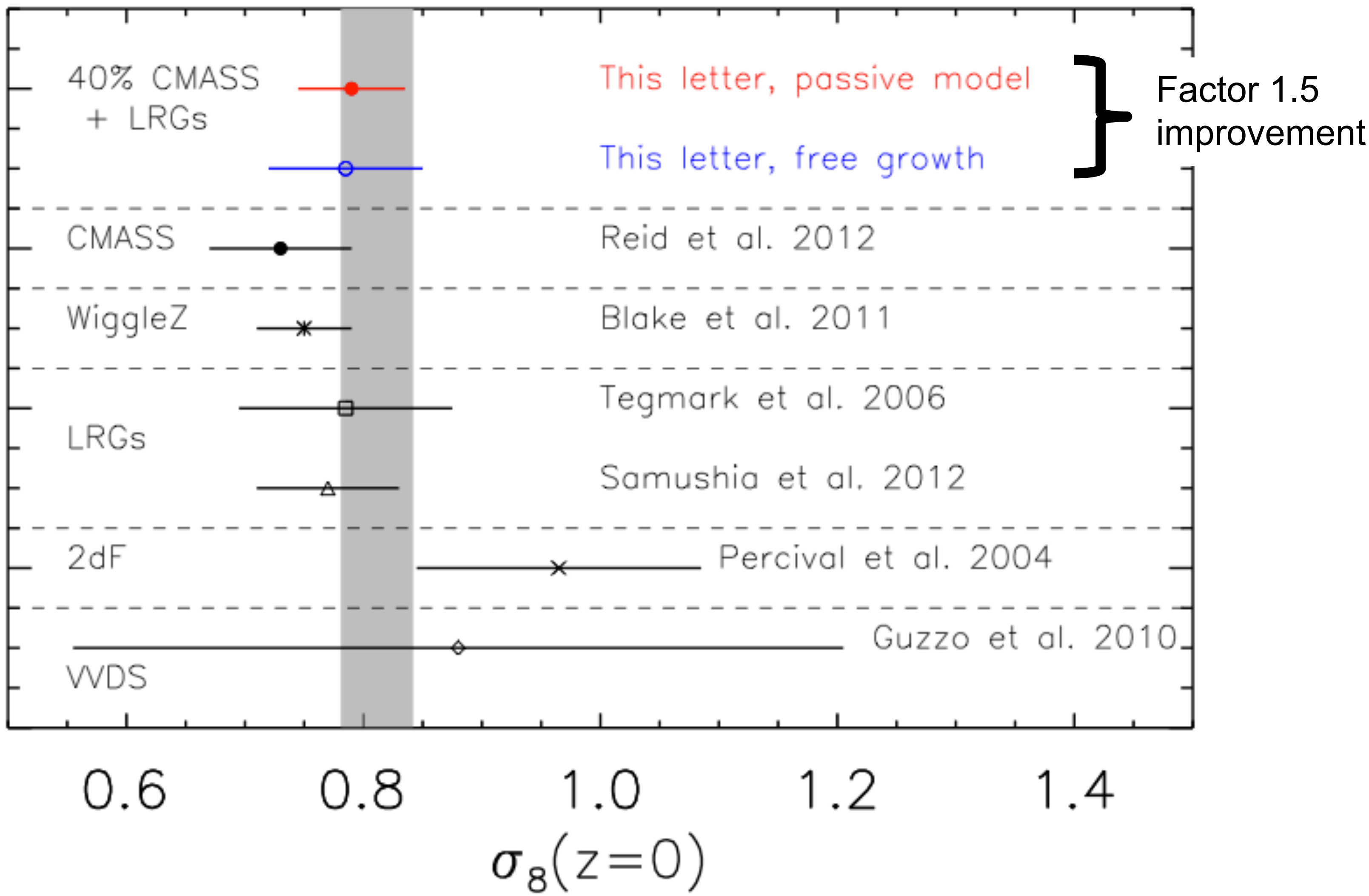

Tojeiro et al.

Fitting the full clustering signal

Fitting the full shape of the correlation function

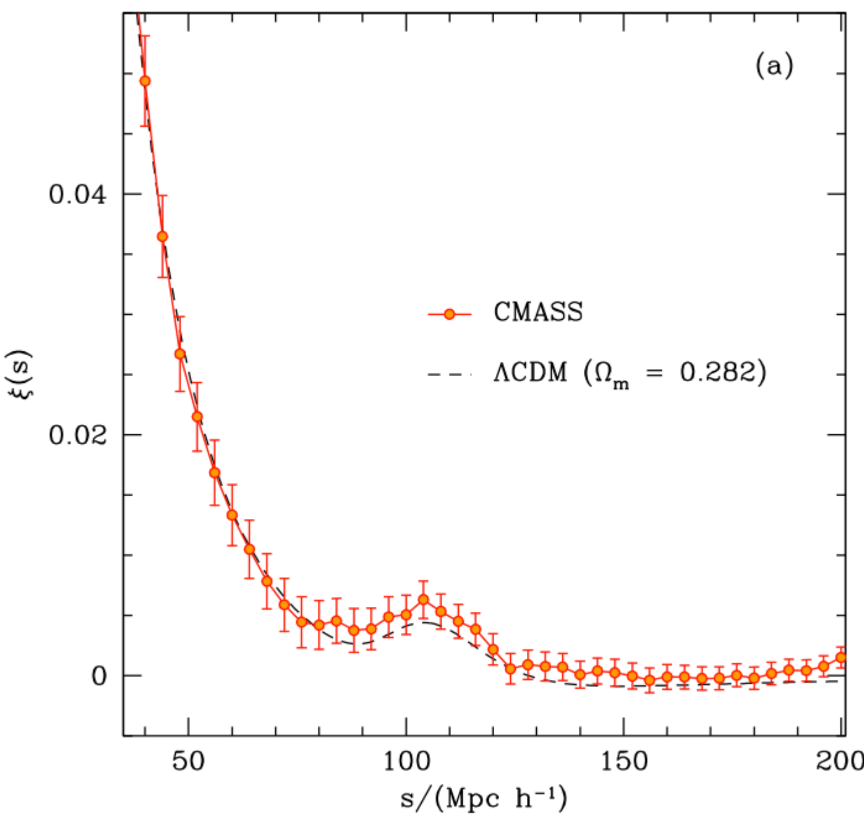

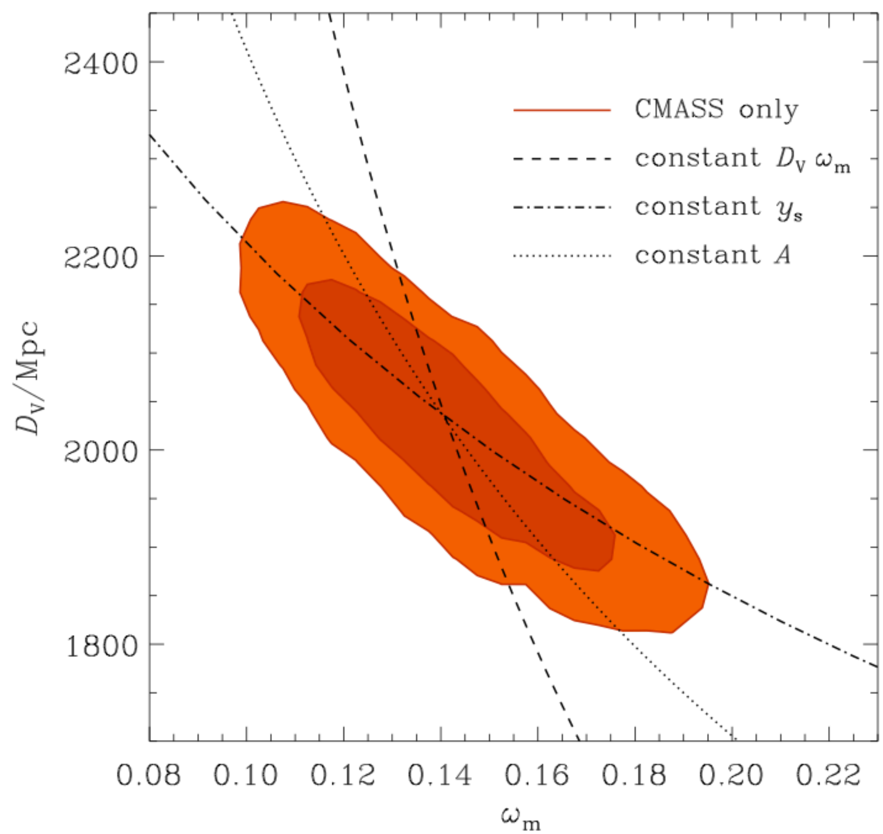

Sanchez et al.

Cosmological constraints from full fit

	CMB	CMB + CMASS	CMB + CMASS +SN	CMB + CMASS +BAO	CMB + CMASS + BAO + SN
w_0	$-1.12^{+0.52}_{-0.51}$	$-1.12^{+0.61}_{-0.58}$	$-1.09^{+0.11}_{-0.11}$	$-0.95^{+0.27}_{-0.27}$	$-1.08^{+0.11}_{-0.11}$
w_a	$-0.3^{+1.2}_{-1.7}$	$0.32^{+0.98}_{-0.99}$	$0.12^{+0.48}_{-0.47}$	$0.05^{+0.62}_{-0.61}$	$0.23^{+0.42}_{-0.42}$
100Θ	$1.0409^{+0.0016}_{-0.0016}$	$1.0409^{+0.0016}_{-0.0016}$	$1.0408^{+0.0015}_{-0.0016}$	$1.0409^{+0.0016}$	$1.0408^{+0.0016}$
$100\omega_b$	$2.219^{+0.042}_{-0.042}$	$2.218^{+0.042}_{-0.041}$	$2.215^{+0.040}_{-0.040}$		
$100\omega_{dm}$	$11.22^{+0.47}_{0.47}$	$11.31^{+0.46}_{-0.46}$	$11.40^{+0.45}_{-0.45}$		
τ	$0.0852^{+0.0061}_{-0.0069}$	$0.0833^{+0.0062}_{0.0067}$	$0.0823^{+0.0058}_{-0.0067}$		
n_s	$0.965^{+0.011}_{-0.011}$	$0.965^{+0.011}_{-0.011}$	$0.963^{+0.011}_{-0.011}$		
$\ln(10^{10}A_s)$	$3.083^{+0.030}_{-0.029}$	$3.082^{+0.030}_{-0.030}$	$3.083^{+0.029}_{-0.029}$		
Ω_{DE}	$0.760^{+0.081}_{-0.087}$	$0.722^{+0.081}_{-0.091}$	$0.730^{+0.016}_{-0.016}$		
Ω_m	$0.239^{+0.087}_{-0.081}$	$0.278^{+0.091}_{-0.081}$	$0.269^{+0.016}_{-0.016}$		
σ_8	$0.87^{+0.12}_{-0.12}$	$0.82^{+0.11}_{-0.11}$	$0.832^{+0.049}_{-0.049}$		
t_0/Gyr	$13.64^{+0.22}_{-0.22}$	$13.79^{+0.16}_{-0.16}$	$13.763^{+0.089}_{-0.091}$		
z_{re}	$10.4^{+1.2}_{-1.2}$	$10.3^{+1.2}_{-1.2}$	$10.2^{+1.2}_{-1.2}$		
h	$0.78^{+0.14}_{-0.14}$	$0.72^{+0.11}_{-0.11}$	$0.712^{+0.020}_{-0.020}$		
$D_V(z_m)$/Mpc	1974^{+86}_{-83}	2040^{+47}_{-45}	2027^{+25}_{-25}		
$f(z_m)$	$0.733^{+0.077}_{-0.078}$	$0.770^{+0.064}_{-0.069}$	$0.766^{+0.022}_{-0.022}$		

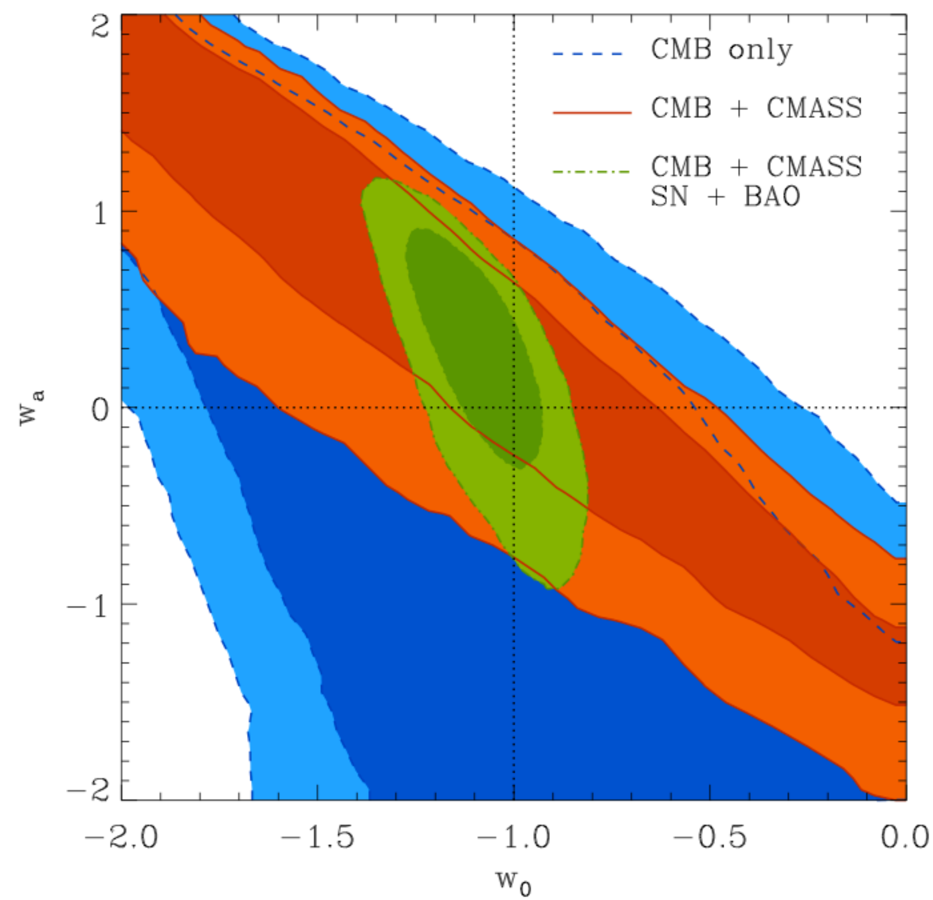

Sanchez et al.

The Future …

SDSS-II LRG clustering

SDSS LRGs at z~0.35

Total effective volume
V_{eff} = 0.26 Gpc^3h^{-3}

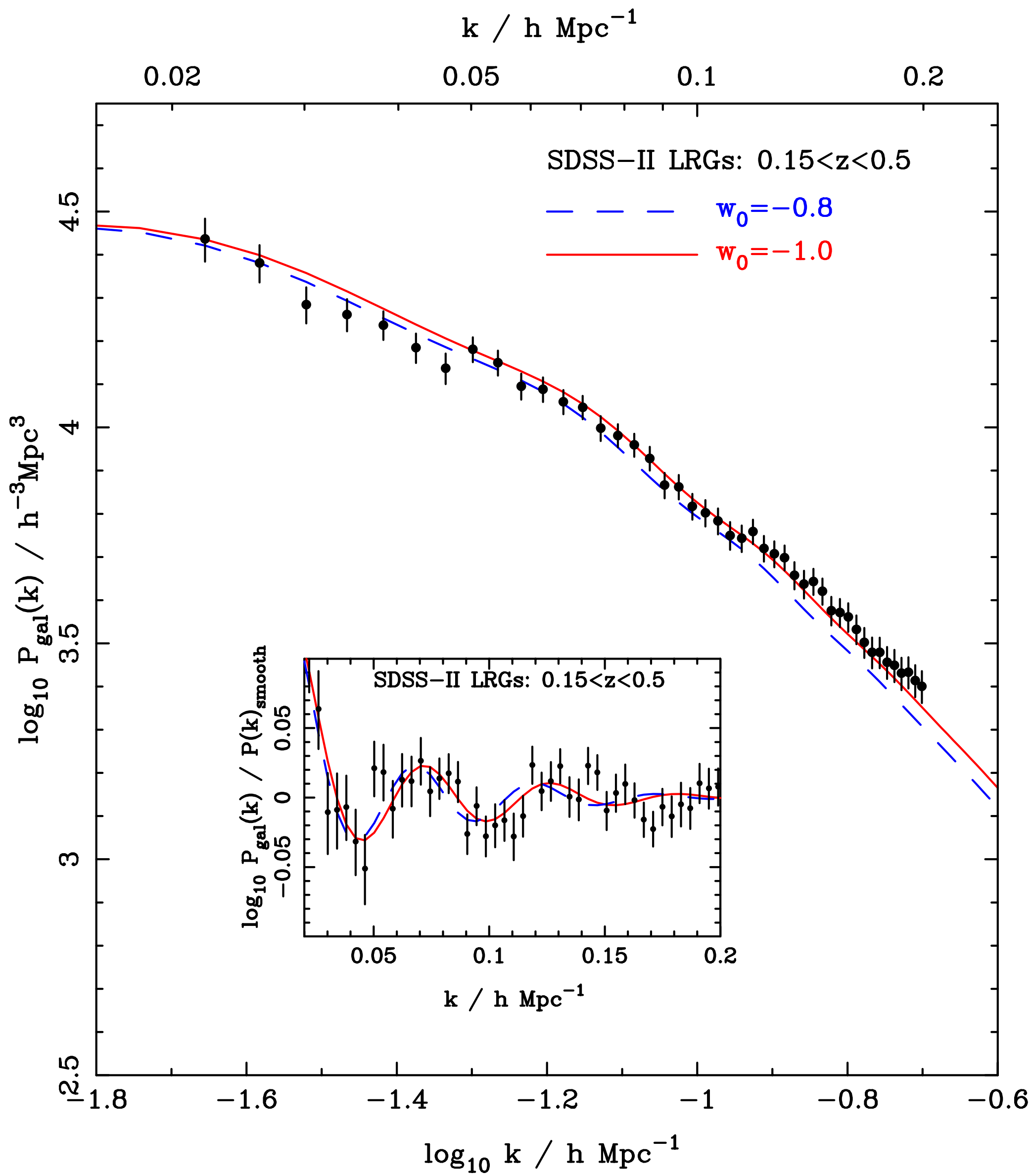

Percival et al. 2009; arXiv:0907.1660

BOSS CMASS DR9 galaxy clustering

BOSS CMASS galaxies at z~0.57

Total effective volume
V_{eff} = 0.77 Gpc^3h^{-3}

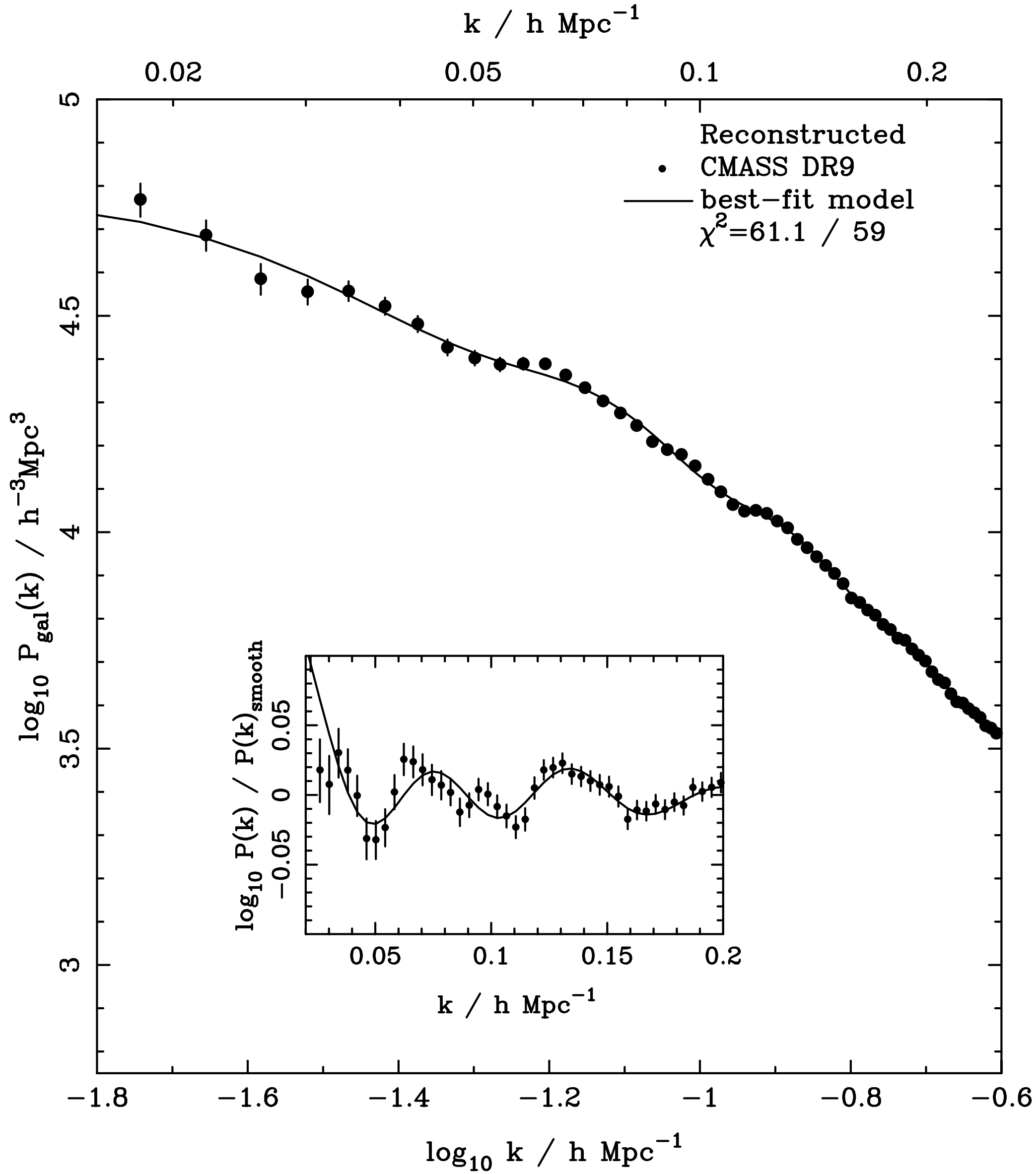

Anderson et al.

Predicted Euclid galaxy clustering

Redshift slice
$0.9 < z < 1.1$

Total effective volume (of Euclid)
$V_{eff} = 19.7\ Gpc^3h^{-3}$

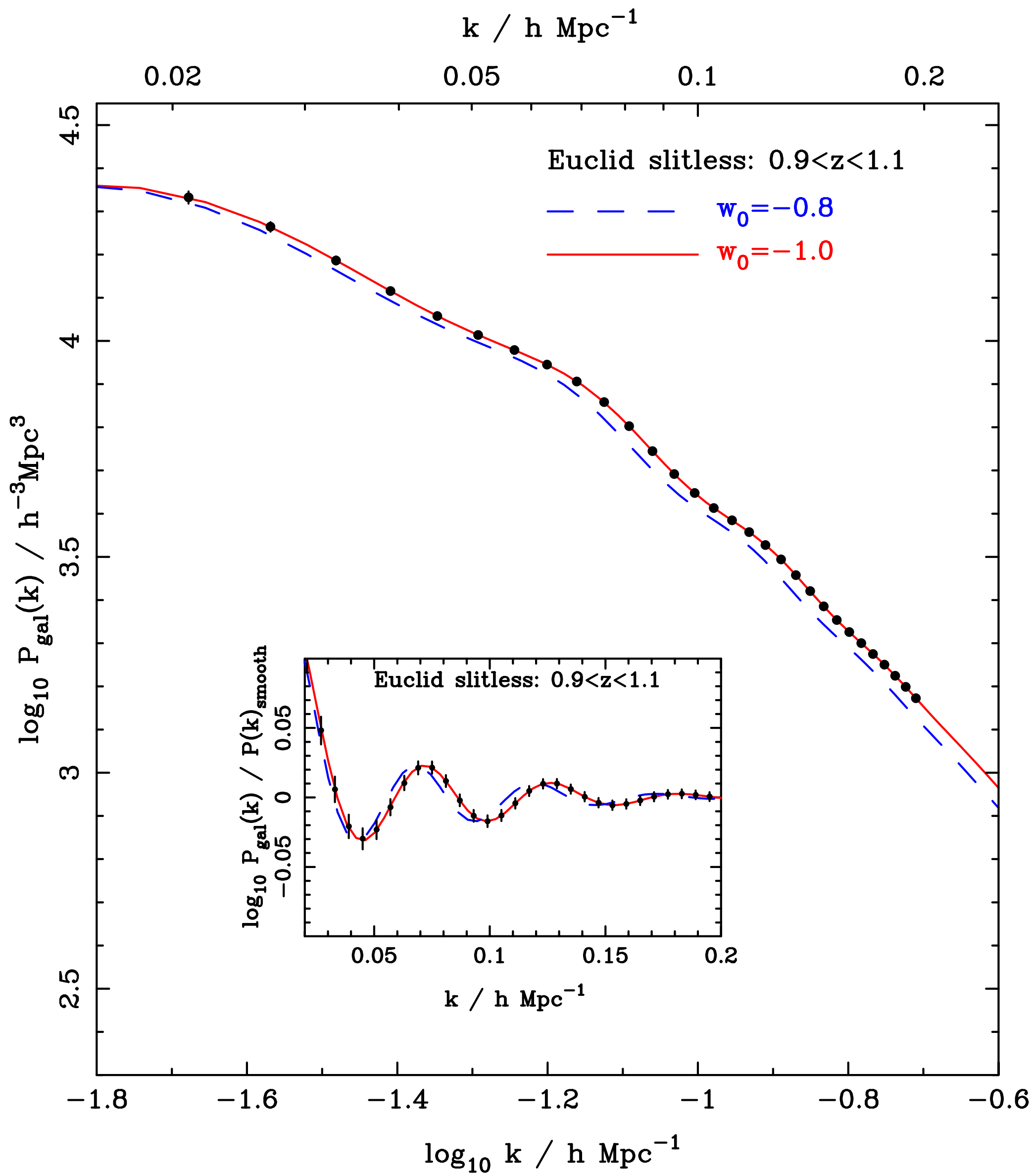

SDSS-II LRG BAO vs other data

ΛCDM models with curvature

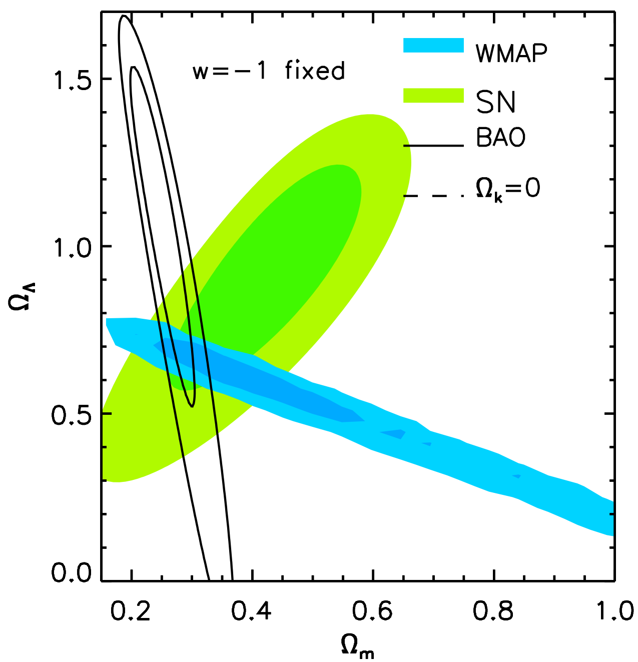

flat wCDM models

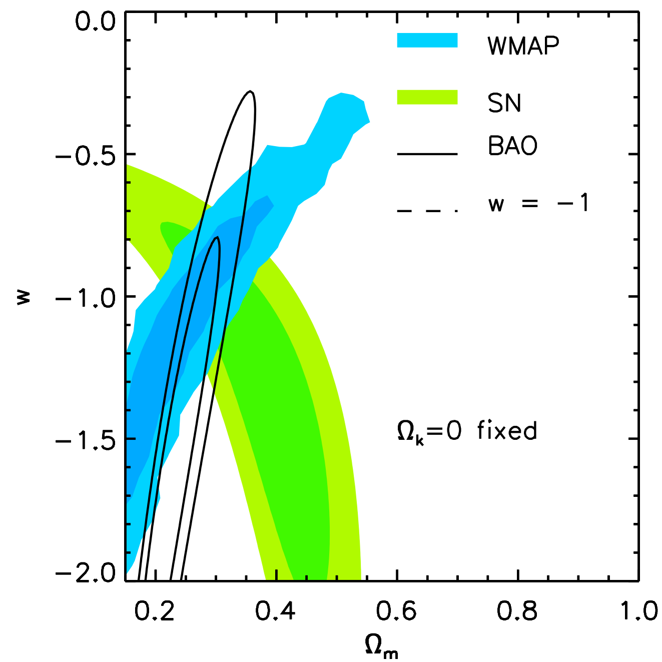

- Union supernovae
- WMAP 5year
- SDSS-II BAO Constraint on $r_s(z_d)/D_V(0.2)$ & $r_s(z_d)/D_V(0.35)$

Percival et al. 2009; arXiv:0907.1660

Euclid BAO predictions

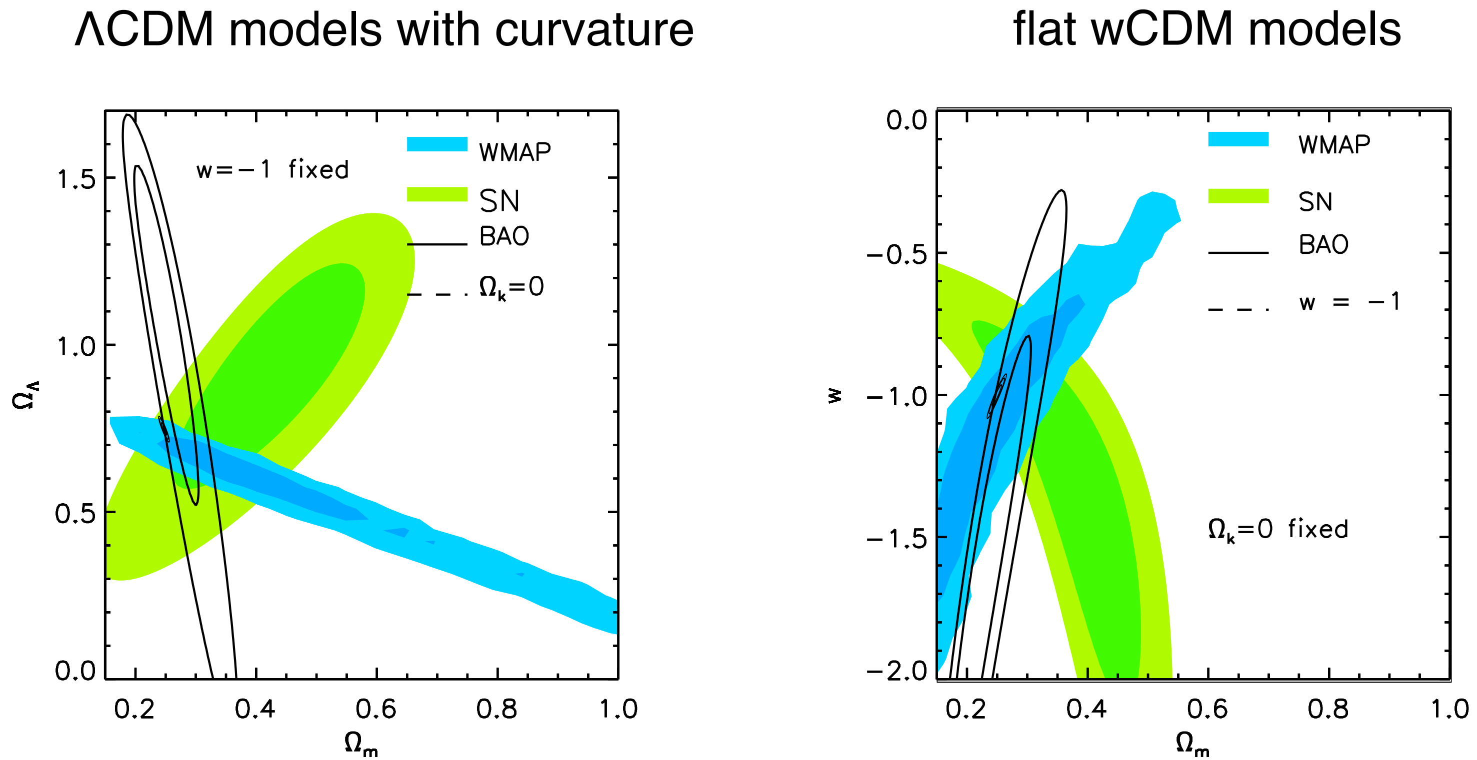

Union supernovae

WMAP 5year

SDSS-II BAO Constraint on $r_s(z_d)/D_V(0.2)$ & $r_s(z_d)/D_V(0.35)$

Conclusions

- Anderson et al. (alphabetical) arXiv:1203.6565
- Reid et al. arXiv:1203.6641
- Sanchez et al. arXiv:1203.6616
- Ross et al. arXiv:1203.6499
- Manera et al. arXiv:1203.6609
- Tojeiro et al. arXiv:1203.6565

- Lots more to come …
  - BOSS DR9 papers on GR implications, fNL, Ω_ν, anisotropic BAO
  - BOSS DR9 is only ~1/3 of the final data set (DR12 Dec 2014)
  - future ground-based surveys (eBOSS, DESpec, BigBOSS, WEAVE, 4MOST)
  - future space-based surveys (Euclid, WFIRST)